May 2004 • NREL/SR-540-35911

Subcontractor Report

Development of the High-Pressure Direct-Injected, Ultra Low-NO_x Natural Gas Engine

Final Report

V.K. Duggal, E.J. Lyford-Pike, and J.F. Wright
Cummins, Inc.
Columbus, Indiana, USA

M. Dunn, D. Goudie, and S. Munshi
Westport Innovations, Inc.
Vancouver, British Columbia, Canada

National Renewable Energy Laboratory
1617 Cole Boulevard, Golden, Colorado 80401-3393
303-275-3000 • www.nrel.gov

Operated for the U.S. Department of Energy
Office of Energy Efficiency and Renewable Energy
by Midwest Research Institute • Battelle

Contract No. DE-AC36-99-GO10337

May 2004 • NREL/SR-540-35911

Development of the High-Pressure Direct-Injected, Ultra Low-NO_x Natural Gas Engine

Final Report

V.K. Duggal, E.J. Lyford-Pike, and J.F. Wright
Cummins, Inc.
Columbus, Indiana, USA

M. Dunn, D. Goudie, and S. Munshi
Westport Innovations, Inc.
Vancouver, British Columbia, Canada

NREL Technical Monitor: M. Frailey

Prepared under Subcontract No. NCI-1-31036-01

National Renewable Energy Laboratory
1617 Cole Boulevard, Golden, Colorado 80401-3393
303-275-3000 • www.nrel.gov

Operated for the U.S. Department of Energy
Office of Energy Efficiency and Renewable Energy
by Midwest Research Institute • Battelle

Contract No. DE-AC36-99-GO10337

NOTICE

Available electronically at http://www.osti.gov/bridge

Available for a processing fee to U.S. Department of Energy
and its contractors, in paper, from:

U.S. Department of Energy
Office of Scientific and Technical Information
P.O. Box 62
Oak Ridge, TN 37831-0062
phone: 865.576.8401
fax: 865.576.5728
email: mailto:reports@adonis.osti.gov

Available for sale to the public, in paper, from:

U.S. Department of Commerce
National Technical Information Service
5285 Port Royal Road
Springfield, VA 22161
phone: 800.553.6847
fax: 703.605.6900
email: orders@ntis.fedworld.gov
online ordering: http://www.ntis.gov/ordering.htm

Printed on paper containing at least 50% wastepaper, including 20% postconsumer waste

Table of Contents

List of Figures

List of Tables

List of Acronyms and Abbreviations

A/F	Air/fuel
ATDC	After top dead center
AVL	Anstalt für Verbrennungskraftmaschinen (Institute for Internal Combustion Engines)
$BSCH_4$	Brake specific methane
BSCO	Brake specific carbon monoxide
BSFC	Brake specific fuel consumption
BSHC	Brake specific hydrocarbons
BSNMHC	Brake specific nonmethane hydrocarbons
$BSNO_x$	Brake specific nitrogen oxides
BSPM	Brake specific particulate matter
BTDC	Before top dead center
BTE	Brake thermal efficiency
CA	Crank angle
CH_4	Methane
CO	Carbon monoxide
CO_2	Carbon dioxide
COV	Coefficient of variance
DoE	Design of experiments
ECM	Engine control module
EGR	Exhaust gas recirculation
EGT	Exhaust gas temperature
EMT	Exhaust manifold temperature
ESC	European Stationary Cycle
ft-lb	Foot-pounds
FTP	Federal Test Procedure
g/bhp-hr	Grams per brake horsepower hour
GRP	Gas rail pressure
GSOI	Gas start of injection
HC	Hydrocarbons
hp	Horsepower
HPDI	High Pressure Direct Injection
HRR	Heat release rate
Hz	Hertz
IDM	Intelligent driver module
IFSM	Integrated fuel supply module
IMEP	Indicated mean effective pressure
IMP	Intake manifold pressure
ISFC	Indicated specific fuel consumption
IVC	Intake valve closure
kW	Kilowatt
L	Liter
mm	Millimeter
MPa	Megapascals
ms	Millisecond
µs	Microsecond
NGNGV	Next Generation Natural Gas Vehicle

N-m	Newton-meter
NMHC	Nonmethane hydrocarbons
NO_x	Nitrogen oxides
NTE	Not-to-exceed
Pd	Palladium
Pivc	Charge pressure at intake valve closure
PM	Particulate matter
Pmax	Maximum cylinder pressure
ppm	Parts per million
PPW	Pilot pulse width
PSOI	Pilot start of injection
Pt	Platinum
PW	Pulse width
RIT	Relative injection timing (equivalent to pilot separation)
RSM	Response surface model
SOF	Soluble organic fraction
SOI	Start of injection
SOL	Solids
SV	Space velocity
TDC	Top dead center
TDM	Test Data Manager (by Schenck-Ricardo)
Tivc	Charge temperature at intake valve closure
ULSD	Ultra-low sulfur diesel
VGT	Variable geometry turbocharger
VIP	Variable injection pressure

1.0 Executive Summary

Natural gas is a domestically available alternative fuel. The U.S. Department of Energy supports natural gas engine and vehicle research and development to help the United States reach its goal of reducing dependence on imported petroleum. Another benefit of natural gas vehicles is that they can reduce emissions of regulated pollutants compared with diesel vehicles. The U.S. Department of Energy supported the work described in this report through its Next Generation Natural Gas Vehicle activity, which is led by the National Renewable Energy Laboratory.

Current medium- and heavy-duty natural gas engines use lean-burn spark ignition technology to achieve low emissions with full-load efficiencies slightly lower than those of diesel engines. Part-load efficiencies, however, are much lower than those of diesel engines.

Westport Innovations Inc.'s High Pressure Direct Injection (HPDI™) natural gas fuel system used in an otherwise unmodified heavy-duty diesel engine reduces nitrogen oxides (NO_x) and particulate matter (PM) emissions while maintaining diesel-like efficiencies at full and part loads. The fuel system directly injects a small quantity of pilot diesel fuel that ignites directly injected high-pressure natural gas.

This project targeted development of a high-efficiency, low-emission natural gas engine for heavy-duty trucks. Specifically, it targeted the demonstration of a Cummins ISX engine using HPDI natural gas fueling and exhaust gas recirculation (EGR) meeting the following specifications:

- Peak torque of 1,650 ft-lb (2,236 N-m)
- Rated power of 450 hp (335 kW)
- Peak thermal efficiency of 40% with typical diesel part-load efficiency
- NO_x emissions of 0.5 g/bhp-hr
- PM emissions of 0.1 g/bhp-hr
- Substitution of diesel with natural gas greater than 90% over the certification cycle

Testing and modeling of an otherwise unmodified Cummins ISX engine with EGR and HPDI fueling indicated that the program goals could not be met with the standard production hardware. Therefore, a turbocharger using a smaller trim compressor and a second EGR cooler were fitted to the engine along with an oxidation catalyst.

Compared with HPDI fueling without a catalyst, the catalyst reduced the AVL 8-mode cycle weighted PM emissions by 34% from 0.04g/bhp-hr to 0.03g/bhp-hr. Nonmethane hydrocarbon (NMHC) emissions were reduced by 54% and carbon monoxide (CO) emissions by 96%.

A steady-state engine calibration was developed using design of experiment test techniques. Testing over the European Stationary Cycle (ESC) 13-mode cycle resulted in weighted NO_x emissions of 0.37 g/bhp-hr, NMHC emissions of 0.2 g/bhp-hr, methane

(CH_4) emissions of 2.08 g/bhp-hr, PM emissions of 0.04 g/bhp-hr, and a weighted thermal efficiency of 36.1% (diesel-equivalent fuel consumption of 173 g/bhp-hr). Peak thermal efficiency was 39.5%, and weighted diesel (pilot) use was 6% of total fuel consumption. At high-load conditions, the pilot quantity accounted for less than 5% of total fuel consumption.

The engine, in its final hardware configuration, was shipped to the Cummins Engine Company, and the transient testing and calibration refinement was conducted at Cummins' facilities. The calibration met the targeted power and torque requirements of 450 hp and 1,650 ft-lb. Average NO_x emissions of 0.6 g/bhp-hr were repeatedly demonstrated over the Federal Test Procedure (FTP) cycle, with a best result of 0.56 g/bhp-hr. Total hydrocarbon emissions were approximately 5 g/bhp-hr, and much of this was assumed to be CH_4. Average PM emissions remained relatively constant at around 0.03 g/bhp-hr, and the average brake thermal efficiency was 34.1%, which is comparable with state-of-the-art diesel engines.

2.0 Introduction

Congress enacted the Clean Air Act Amendments of 1990 in response to continuing concern about air pollution. The Act's provisions will force broad changes in fuels and vehicles. For example, clean diesel, reformulated gasoline, and alternative fuels are now receiving wide attention as industry tries to comply with the Act. Many ozone non-attainment areas are focusing on heavy-duty alternative fuel vehicles for their State and Federal Implementation Plans because these vehicles have the potential to greatly reduce particulate matter (PM) and nitrogen oxides (NO_x) emissions. Also, alternative fuels may be easier to introduce for fleet-based heavy-duty vehicles because these vehicles often use central refueling depots.

Many technologies must be developed further to take full advantage of the properties of alternative fuels and to enable their widespread use. These include technologies for emissions control, increased energy efficiency, fuel-specific engine optimization strategies, and engine and fuel system hardware. The goal is to develop technologies that will make alternative fuels commercially competitive with diesel in terms of energy efficiency, performance, durability, driveability, cold-start ability, safety, and range, while having an emissions benefit.

Natural gas is a domestically available alternative fuel. The U.S. Department of Energy supports natural gas engine and vehicle research and development to help the United States reach its goal of reducing dependence on imported petroleum, as outlined in the Energy Policy Act of 1992. Another benefit of natural gas vehicles is that they can reduce emissions of regulated pollutants compared with diesel vehicles. The U.S. Department of Energy supported the work described in this report through its Next Generation Natural Gas Vehicle (NGNGV) activity, which is led by the National Renewable Energy Laboratory.

One goal of the NGNGV activity is to develop advanced, commercially viable, medium- and heavy-duty natural gas engines and vehicles that will achieve the U.S. Environmental Protection Agency's 2007/2010 heavy-duty emission levels before 2007. Another goal is to develop production-intent natural gas engines that meet current emission levels and

can be deployed commercially in the near term to gain immediate petroleum displacement and emission reduction benefits. The NGNGV activity is also supported by the South Coast Air Quality Management District and the California Energy Commission.

Current state-of-the-art medium- and heavy-duty natural gas engines employ lean-burn spark-ignition technology to achieve significant emissions reductions while maintaining full-load efficiency marginally lower than diesel engines. Because most of these natural gas engines originated as diesel engines, most are turbocharged and inherently have high cylinder pressures and high power density capability. Lean-burn spark-ignition engine technology lends itself well to these engines. However, current state-of-the-art natural gas engines suffer large efficiency penalties at part load and lesser penalties at full load compared with their diesel counterparts. There are three main reasons for this efficiency penalty in lean-burn spark-ignited natural gas engines: a lower knock-limited compression ratio; the inability to operate at very lean air/fuel ratios at low loads; and, leading to the third reason, the need to use a throttle at part load to limit air flow. These factors greatly influence thermal efficiency and, thus, vehicle operating cost and range.

Westport Innovations Inc.'s High Pressure Direct Injection (HPDI) natural gas fuel system can be used in an otherwise unmodified heavy-duty diesel engine to reduce NO_x and PM emissions while maintaining diesel-like power and efficiency at full and part loads [1,2]. The fuel system directly injects a small quantity of pilot diesel fuel that ignites directly injected high-pressure natural gas. The fuels are directly injected into the cylinder using a single fuel injector with concentric needles and separate injection holes for each fuel.

Exhaust gas recirculation (EGR) reduces NO_x in heavy-duty diesel engines. However high EGR rates can lead to increased PM emissions. Because directly injected natural gas has a lower propensity to form PM emissions than does diesel fuel, it is a good candidate for use with EGR. This report presents some of the development work combining EGR with the Westport HPDI natural gas fuel system on a Cummins ISX heavy-duty diesel engine.

2.1 Project Objectives

This project targeted the development of a high-efficiency, high-performance natural gas engine for heavy-duty trucks that can meet very low NO_x emissions levels. Specifically, the project targeted the demonstration of a Cummins ISX engine using HPDI natural gas fueling and EGR meeting the following specifications:

- Peak torque of 1,650 ft-lb (2,236 N-m)
- Rated power of 450 hp (335 kW)
- Peak thermal efficiency of 40% with typical diesel part-load efficiency
- NO_x emissions of 0.5 g/bhp-hr
- PM emissions of 0.1 g/bhp-hr
- Substitution of diesel with natural gas greater than 90% over the certification cycle

3.0 Engine Development and Evaluation

3.1 Engine and Test Cell

Engine Description

The Cummins ISX (Figure 1) is a six-cylinder 15 L heavy-duty engine with a 17:1 compression ratio. The engine uses a high-pressure EGR loop (Figure 2) that includes a variable geometry turbocharger (VGT), EGR valve, and EGR cooler. Engines are commercially available with ratings of 400-565 hp. The engine used in this work was rated at 450 hp (335 kW) and 1,650 ft-lb (2,236 N-m).

Figure 1: ISX Engine

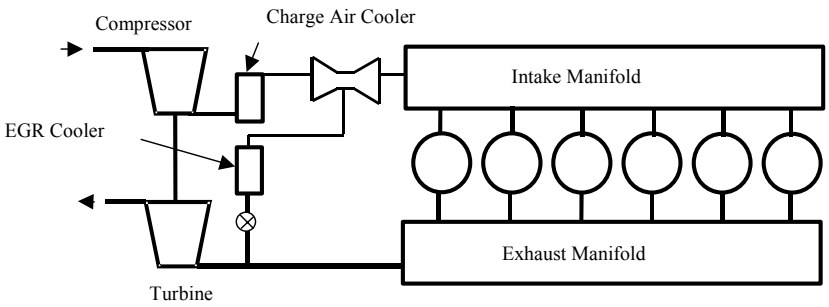

Figure 2: High-Pressure EGR Loop Schematic

The ISX engine with EGR was made commercially available in October 2002. This project began in 2001 before production engines were available, so initial work was conducted with a pre-production engine. A production ISX was used for later testing and final calibration. There were no fundamental hardware differences between these two engines, only changes to improve durability and robustness of controls. Therefore, the original modeling and test work using the pre-production engine was directly applicable to the production engine.

Test Cell Description

The test cell was fitted with equipment and services suitable for the ISX engine, including the following:

- AVL B-500 eddy current dynamometer with 480 kW capacity
- Meriam laminar flow element for air flow measurement
- Micro-Motion gas flow meter
- Gravimetric diesel fuel measurement system (pail and scale)
- Water-cooled charge air heat exchanger
- Water-cooled engine coolant heat exchanger
- Agilent Micro Gas Chromatograph for natural gas composition analysis
- AVL opacimeter
- Digalog data acquisition and controls system

An additional diesel fuel supply system was installed for ultra-low sulfur diesel (ULSD). This fuel has a sulfur content of less than 15 ppm to prevent the poisoning of exhaust catalysts. The ULSD will be used during future aftertreatment research.

The engine instrumentation included in-cylinder high-speed pressure transducers on all six cylinders. The transducers on cylinders 1 and 6 are flush-mounted to the fire deck and water cooled. Those on cylinders 2 through 5 are side mounted and separated from the combustion chamber by a drilled passage. Low-speed pressure and temperature sensors were installed at all necessary locations in the intake, charge air, EGR, and exhaust lines.

Emissions were measured with a Horiba 7500D-EGR exhaust gas analyzer. This system can monitor pre- or post-catalyst exhaust emissions and the carbon dioxide (CO_2) concentration in the engine intake manifold to determine EGR rates. PM is measured using a gravimetric method and a mini-dilution tunnel from Sierra Instruments. The engine and test cell are shown in Figure 3.

Figure 3: Test Cell with ISX Engine

Test Cell: Data Acquisition and Post-Processing

Three separate data streams are recorded in the test cell:

- General test cell instrumentation, using the Digalog system
- Engine parameter information, recorded from the engine control module (ECM)
- High-speed in-cylinder pressure measurements, using an AVL 619 Indiset

All data were typically collected at a 1-Hz sampling frequency, except for the in-cylinder pressure measurements, which were recorded at a 0.5-degree crank angle (CA) resolution. Probes at the entrance to the inlet manifold, to sample the CO_2 concentration

for calculation of the EGR rate, are shown in Figure 4. Later, when the engine was replaced, CO_2 samples were taken along the intake manifold near the intake valves. A Cummins electronic calibration tool records ECM data such as fueling and timing commands and EGR system control settings, which cannot be directly recorded by the main data acquisition system.

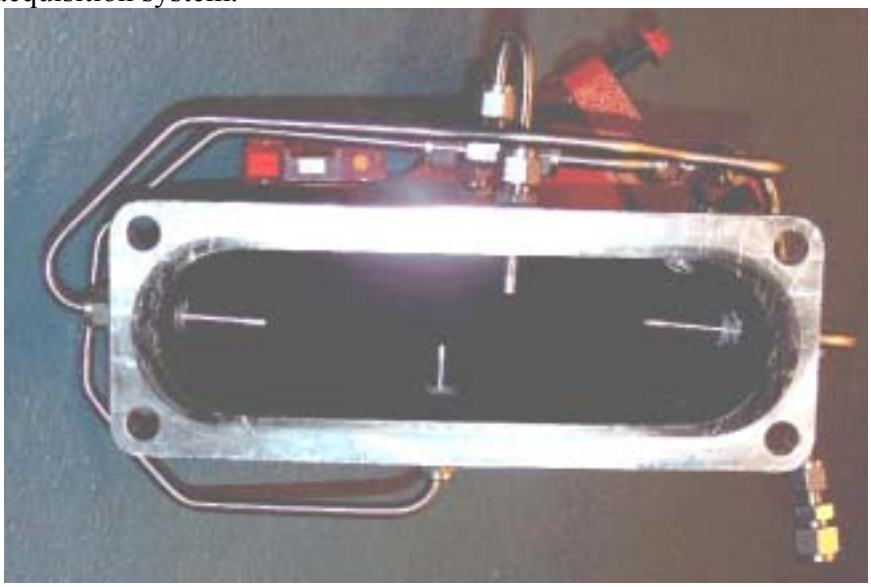

Figure 4: CO_2 Sampling Probes for Inlet Charge EGR Measurement

Data are typically recorded for 3 minutes. The test cell data and the ECM data are combined and processed using the software package Test Data Manager (TDM) by Schenck-Ricardo. TDM is an integrated data storage and processing tool that is secure and follows a quality assurance procedure to ensure that any changes are traceable. TDM cannot process high-speed data at present, so these are processed separately.

Test Cell: Validation

The engine was installed, broken-in and tested at Cummins Engine Company using a 565-hp calibration. The calibration was then changed to 450 hp, and an AVL 8-mode test was conducted. This same test was then performed at Westport to validate the Westport test cell. Comparison of these results showed that all instrumentation was functioning as required except for one intake manifold pressure sensor. This was replaced, and subsequent measurements were comparable to the Cummins measurements. Also, two test runs were conducted at Westport to check repeatability. As a result, the fuel mass measurement technique was modified to make the results more robust. With these few improvements, the test cell and engine were considered to be in good health. Data quality was monitored continuously during the test program.

3.2 Modeling and Analysis

3.2.1 Objective

Analyses of combustion and engine performance were conducted with the following objectives:

- Develop a model to help understand combustion processes and predict the effect of EGR on NO_x emissions and engine performance
- Anticipate the capability of the engine hardware to achieve the EGR levels needed to meet the targeted NO_x emissions
- Anticipate the engine settings required to meet the targeted NO_x level

The combustion/NO_x model and the engine performance model were validated using test data. The analytical tools will also be used during the engine testing phase to assist optimization.

3.2.2 Accomplishment Summary

An engine performance model was developed using GT-Power. The model was validated using test data with and without EGR under diesel and HPDI fueling. A combustion model (XPNOx) for NO_x emissions was also developed at Westport. It is a multi-zone combustion model that calculates heat release rate and NO_x based on in-cylinder pressure traces. XPNOx was validated using test cell data with and without EGR under diesel and HPDI fueling. Both were found to predict engine performance well with some limitations.

After validation, both models were used to predict the EGR rates, engine settings, and capability of the engine to meet the NO_x emissions target of 0.5 g/bhp-hr. Hardware deficiencies were identified, and suggestions for improvements were made. The suggested hardware changes included a smaller trim compressor and an extra EGR cooler. Using this new hardware, the models identified the likely engine settings to reach the 0.5 g/bhp-hr NO_x emissions target.

3.2.3 Accomplishment Details

<u>GT Power: Engine Performance Model</u>

GT-Power is a commercially available computer program that predicts engine performance. It can calculate performance data such as air flow rate, fuel flow rate, brake torque and power, brake mean effective pressure, intake manifold pressure, cylinder pressure versus CA, residual gas fraction, brake specific fuel consumption (BSFC), brake thermal efficiency (BTE), volumetric efficiency, heat release rate, mass burn profile, wall heat transfer, compressor/turbine work, and more. A GT-Power model of the six-cylinder Cummins ISX-EGR engine with a VGT was developed (Figure 5).

<u>GT-Power: Engine Model Validation</u>

Much of the steady-state engine testing was conducted over the AVL 8-mode test cycle, so the engine model was validated at these points (Figure 6). Modeling and validation were conducted with increasingly complex models:

- Diesel fuel only without EGR
- HPDI without EGR
- Diesel fuel only with EGR
- HPDI with EGR

This progression enabled successive validation of the base engine, EGR system, and HPDI fuel system models. The model was found to be a good predictor of actual engine performance at most conditions with some minor limitations. The model was not highly accurate at low fueling (idle) or conditions near the extremes of the turbocharger map.

With some limitation at low-power conditions, the model allows the prediction of the effects of major changes, such as changes to turbocharger characteristics, EGR rates, start of injection (SOI) timing, and so forth.

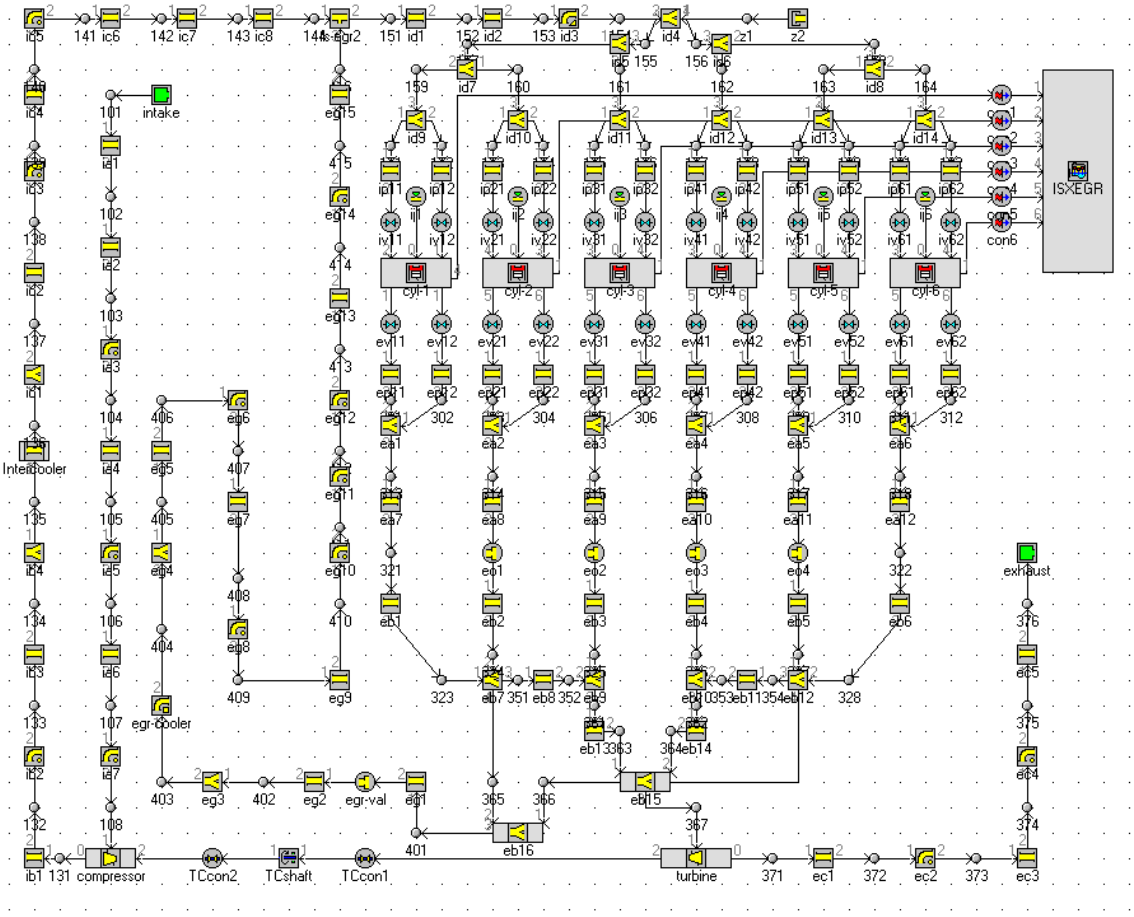

Figure 5: GT-Power Engine Simulation Model Layout for the ISX-EGR Engine with VGT

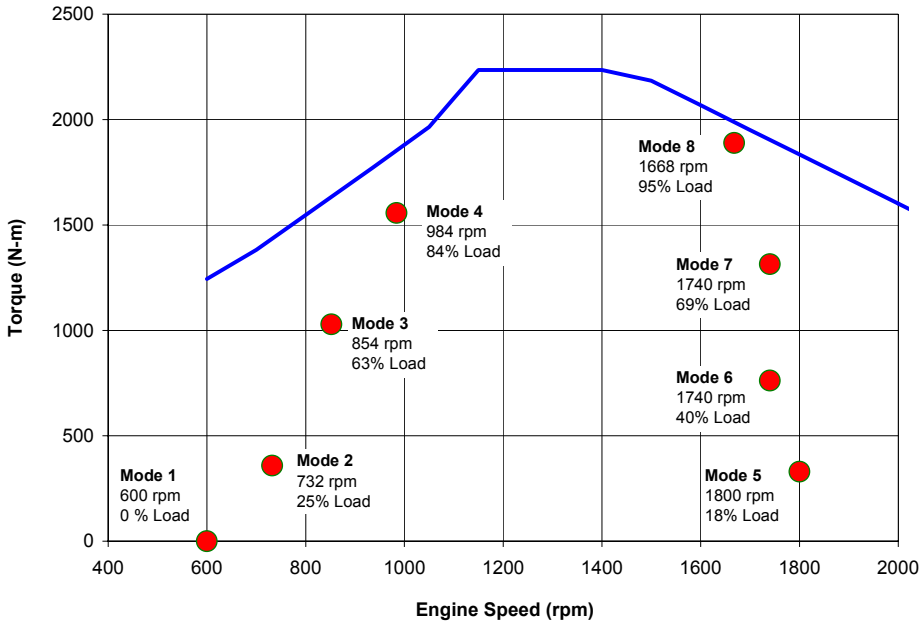

Figure 6: AVL 8-Mode Test Points and 450 Hp/1,650 ft-lb (335 Kw/2,236 N-m) Torque Curve

XPNOx: Combustion Model

XPNOx is computer program developed by Westport to estimate NO_x emissions. Based on actual cylinder pressure data from an engine test, it calculates the heat release rate, temperature, and resulting rate of NO production in each of many zones of burned gas.

Combustion in each gas packet is stoichiometric, with a separate combustion zone created for each CA degree. NO is generated according to the extended Zeldovich mechanism in each burned zone for a period of one "turbulent mixing time" after burning; after this, instantaneous mixing with unburned gas freezes the NO level. Experience with non-EGR ISX engines indicates that a turbulent mixing time of 0.6 ms characterizes NO formation over a wide range of conditions for both diesel and natural gas fueling. As the model evolved, a 0.3-ms mixing time was found to provide better predictions. After mixing, each burned-and-mixed zone expands to successively lower pressures and temperatures. The residual gas fraction is determined by satisfying mass and energy balances at inlet valve closure.

Calculated NO is sensitive to end-of-compression temperature, so the compression curve is corrected as necessary to have reasonable consistency with polytropic compression. A polytropic exponent is calculated from the variable-specific heat isentrope and a heat transfer estimate based on the Woschni correlation. Measured cylinder pressures are erratic at inlet valve closure, so end-of-compression temperature is best estimated by comparing measured and calculated polytropes at the upper end of the compression curve.

XPNOx: Model Validation

XPNOx was validated at common points on the AVL 8-mode or European Stationary Cycle (ESC) 13-mode tests, with diesel and HPDI fueling, both with and without EGR. Only the HPDI results are presented here.

For validation against real engine results, the XPNOx model was run at various AVL modes and its predictions compared with measured data. Figure 7 shows that these agreed well at modes 3, 4, 6, 7, and 8, with errors under 20%. The model was off by about 80% at mode 5. The predicted mode-weighted NO_x based on numerical results from modes 3-8 was within 10% of the engine. The model uses cylinder pressure data from cylinder 1 only. This approach is reasonable as long as all six cylinders have nearly identical pressures. However, in some cases significant cylinder-to-cylinder variations may occur owing to differences in the injection timing and EGR distribution.

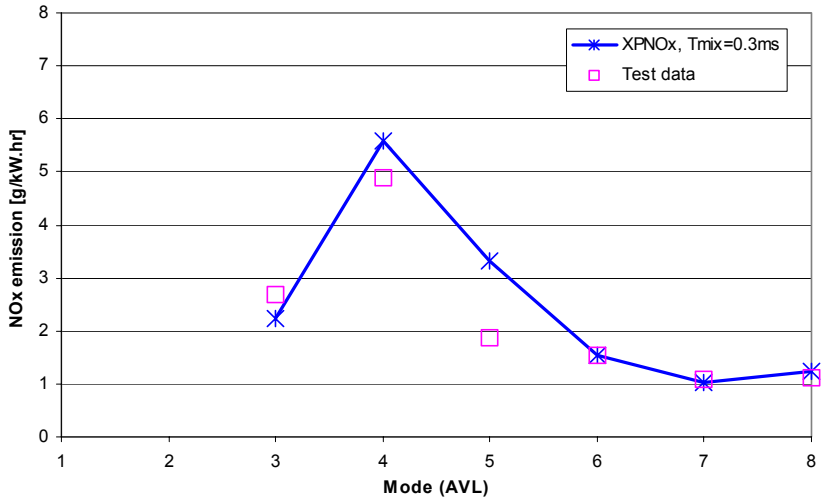

Figure 7: NO_x Emissions Prediction Compared with Measurements for AVL Modes 3-8

XPNOx did not give meaningful results at modes 1 and 2 because the computer program fails to converge to a solution at low loads, perhaps owing to errors in the inputs. Because the vast majority of cycle NO_x is from modes at which XPNOx operates well, the tool will be useful for concept-level work. More accurate measurements of EGR flow, cylinder pressure, air/fuel ratio, fueling rate, and fuel injection timing will likely improve the stability of the code at low load. Although not exact, the validated XPNOx model will be a useful predictor of NO_x emissions.

Investigation of EGR Maldistribution

EGR maldistribution between cylinders could adversely affect engine optimization. It also affects the accuracy of the NO_x prediction model because the model assumes a uniform EGR rate for all cylinders. EGR maldistribution has two causes: 1) poor mixing between the EGR and intake air, and 2) The effects of cylinder firing order and pressure pulsations in the intake and exhaust manifolds. The second effect was quantified using GT-Power at AVL modes 3, 5 and 8 (Figure 8). Even if perfect mixing between air and

EGR is assumed, cylinder phasing and pressure pulsations are likely to contribute about 1%-3% variation in the EGR rate between the cylinders.

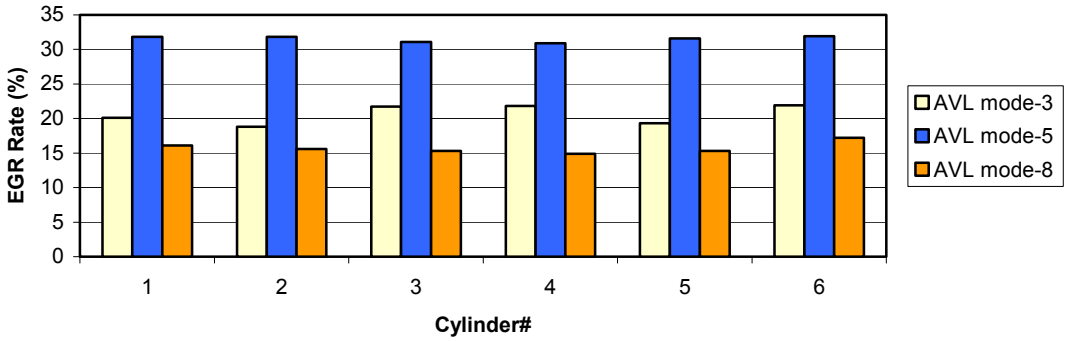

Figure 8: Distribution of EGR Between Cylinders at AVL Modes 3, 5, and 8

Investigation of Shortened Heat Release at High Load

Engine test data at AVL mode 8 show a long tail on the heat release, indicating that the combustion period is too long; this will hurt the engine fuel efficiency. GT-Power was used to assess the effect of faster combustion on engine performance and efficiency. Two cases were run: 1) original rate of heat release from test data, and 2) modified rate of heat release with the combustion tail cut at 60-degrees CA after top dead center (ATDC). The profiles used are shown in Figure 9.

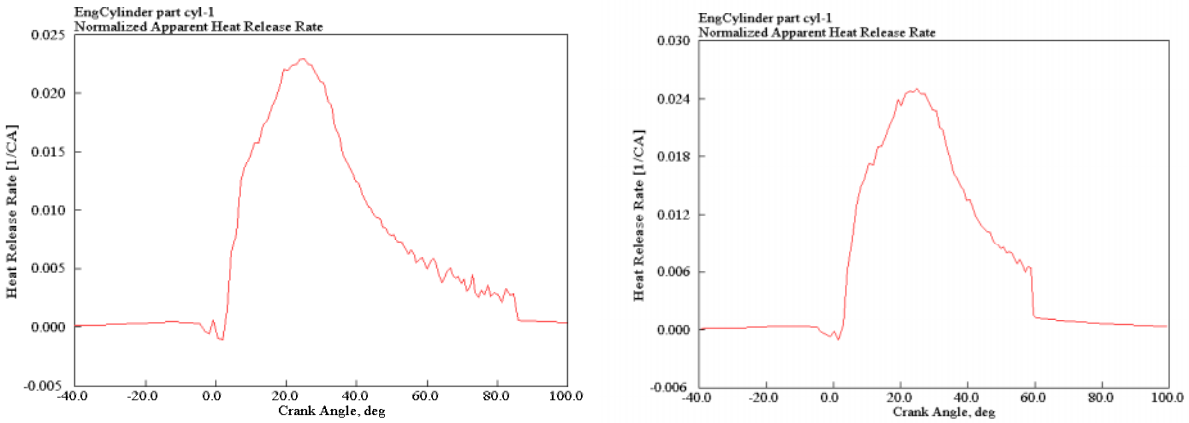

Figure 9: Original and Modified Rate of Heat Release Profile at AVL Mode 8

The shorter heat release period resulted in a 4% increase in engine indicated mean effective pressure (IMEP) and a 5% decrease in indicated specific fuel consumption (ISFC). The EGR rate was almost unchanged. The peak cylinder pressure increased by 2.3%. This suggests that it is beneficial to reduce the "tail" of the heat release.

Investigation of Smaller Compressor Trim

At AVL mode 4 (984 RPM, 84% torque), the engine was found to be operating very close to the compressor surge limit, resulting in instabilities in the air handling controls.

This is aggravated when the EGR rate is increased by closing the VGT turbine ring gap. One option is to try a smaller compressor to move the operating point away from the surge line. The GT-Power model was run at AVL mode 4 with two different compressor maps. As seen in Figure 10, a smaller compressor moved the operating point away from the surge line. The predicted IMEP, ISFC, and EGR are unchanged. A smaller compressor will allow better VGT control and higher EGR rates.

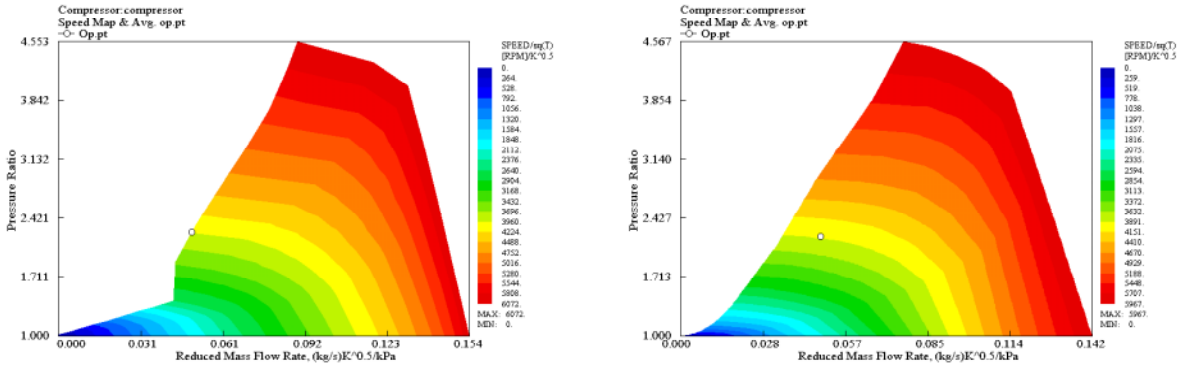

Figure 10: Original and Smaller Compressor Speed Maps with AVL Mode 4 Operating Point

As a next step, the model was run with the smaller compressor at AVL mode 8 to assess its suitability at high load. The result is shown in Figure 11. The engine performance was unchanged, but the operating point moved further away from the surge line. These results suggest the engine would benefit from using a smaller trim compressor.

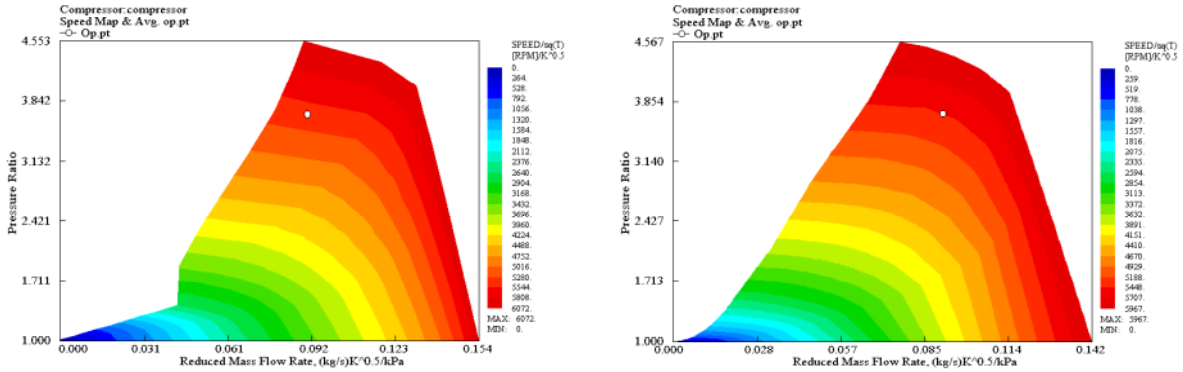

Figure 11: Original and Smaller Compressor Speed Maps with AVL Mode 8 Operating Point

Effect of VGT Turbine Rack Position on EGR Rate

The turbocharger has a variable turbine nozzle ring gap that changes the flow area inlet to the turbine. One method of driving more EGR is to vary this ring gap. By reducing the ring gap, the exhaust pressure in increased, which drives more EGR. However, the compressor also spins faster and drives more fresh air. The GT-Power model was run at different ring gap positions at AVL mode 8 to assess the effects. In Figure 12, the EGR

rate increases to 25% as the turbine ring gap is closed. The IMEP and ISFC are unchanged.

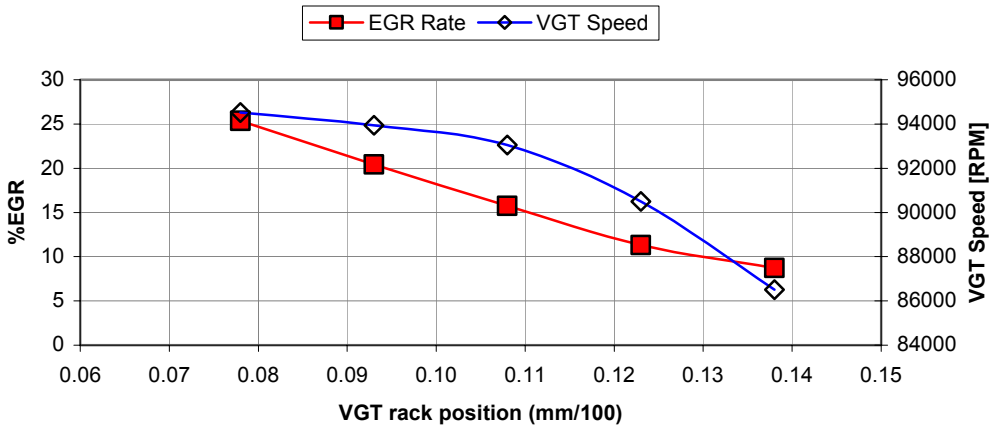

Figure 12: Effect of Turbine Ring Gap (Rack Position) at AVL Mode 8 on EGR Rate and VGT Speed

The effect of closing the ring gap on the compressor operating point is shown in Figure 13. The standard compressor will be surge limited when trying to drive high EGR rates even at the highest engine speeds.

The GT-Power model was also run at AVL mode 4 to see the effect of turbine ring gap on EGR rate and engine performance. In this case, the engine was modeled with the smaller compressor shown in Figure 11 to bring the compressor away from the surge line.

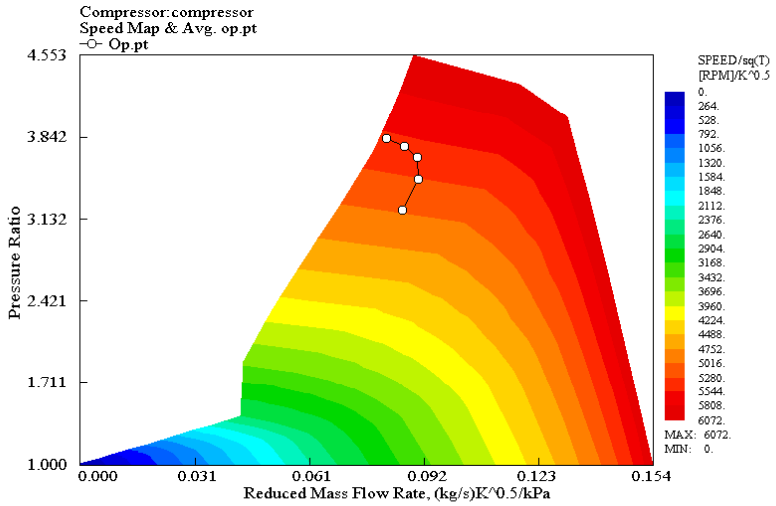

Figure 13: Standard Hardware Compressor Speed Map and Operating Points at Various Turbine Ring Gaps (at AVL Mode 8)

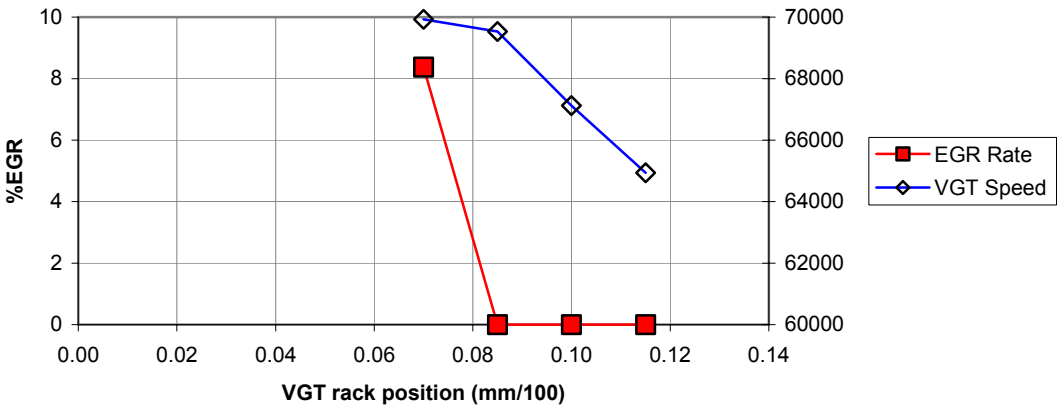

Figure 14: Effect of Turbine Ring Gap (Rack Position) on EGR Rate and Cylinder Peak Pressure with Smaller Compressor Trim (at AVL Mode 4)

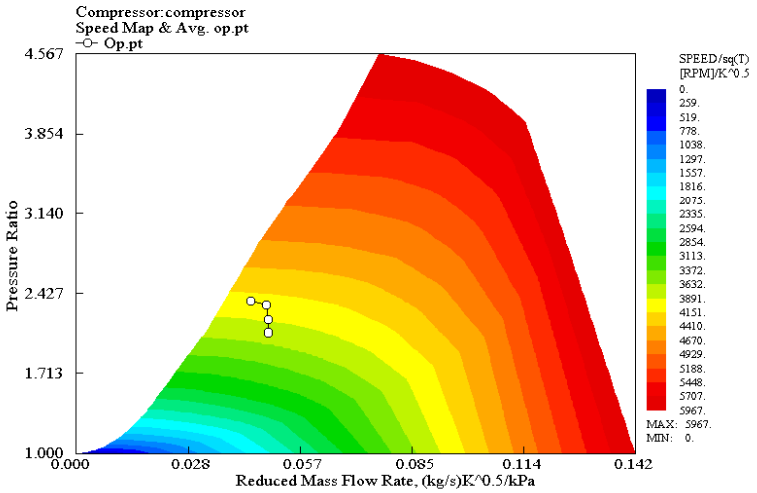

Figure 15: Smaller Trim Compressor Speed Map and Operating Points at Various Turbine Ring Gaps (at AVL Mode 4)

In this case (Figure 14), the EGR rate remained zero until the ring gap was closed below 0.085. It increased to about 8% at a ring gap of 0.07 (i.e., 7 mm gap). The compressor map (Figure 15) shows that the smaller compressor provides sufficient surge margin even when the rack is closed and the mass flow rate through the compressor is reduced. The IMEP and ISFC are unchanged.

Effect of a Larger EGR Valve on EGR Rate

With a fixed VGT setting and the EGR valve fully open at AVL mode 8, the EGR rate is 15%. The current EGR valve is 44 mm in diameter. The GT-Power model was run with a larger EGR valve (50 mm, 30% more flow area) at the same operating conditions. As seen from Figure 16, a 30% increase in EGR valve flow area does not increase the EGR rate appreciably. The existing EGR valve size is sufficient and is not limiting the EGR rate.

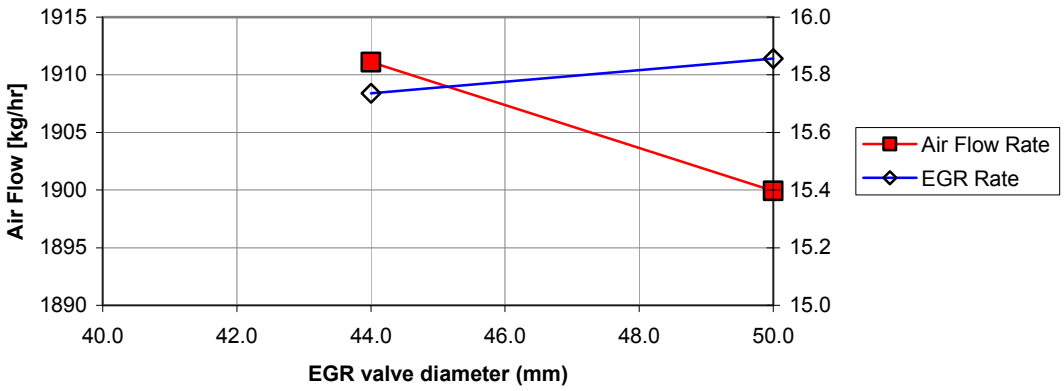

Figure 16: Effect of EGR Valve Diameter on Airflow Rate and EGR Rate at AVL Mode 8

Effect of a Smaller Turbine

The ISX engine has several ratings from 400-565 bhp. The standard VGT turbine is sized to allow operation up to the highest rating, but it may not be the best choice at lower power (450 bhp) and higher EGR rates. The engine model was run at AVL mode 8 with different turbines by scaling the turbine map with factors of 0.8, 1.0 (baseline), and 1.2. A factor of 0.8 applied to the turbine mass flow rate simulates a smaller turbine, which increases the EGR rate from 16% to 27%. IMEP and ISFC are unchanged. Comparing Figure 17 and Figure 18 with earlier results (Figure 12 and Figure 13) shows that the effect is similar to closing the turbine ring gap.

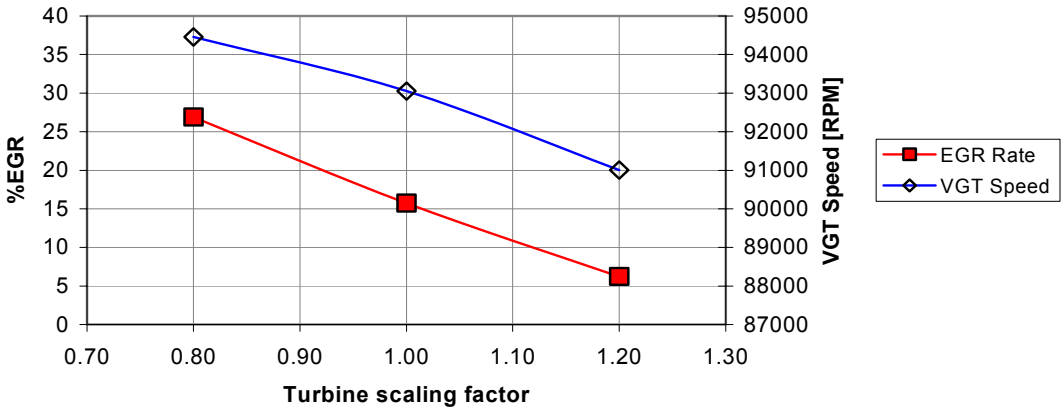

Figure 17: Effect of VGT Turbine Size on EGR Rate and VGT Speed at AVL Mode 8

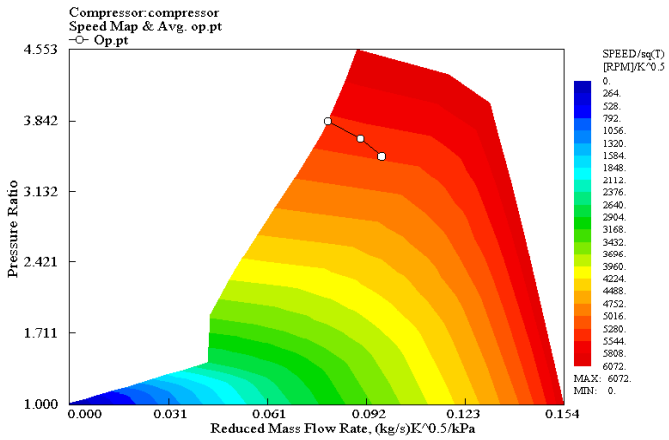

Figure 18: Effect of VGT Turbine Size on the Compressor Operating Point at AVL Mode 8

EGR Introduction: Comparison Between a Venturi and Reed Valve

Presently, the ISX uses a venturi in the inlet system to draw in EGR from the exhaust. However, pressure pulsations in the exhaust can be used to introduce EGR into the inlet system via a reed valve. In a six-cylinder, four-stroke engine there are six pressure pulses in the exhaust system per engine cycle and two revolutions per cycle. A reed valve leading to the inlet manifold would open briefly during each exhaust pressure pulse, sending EGR into the inlet. To study this alternative, the engine was modeled with a reed valve at AVL mode 8, and the results were compared with a standard model with the venturi. The EGR valve was kept fully open in both cases. The venturi and the reed valve provided very similar EGR rates (~ 19%) and identical IMEP and ISFC. There is no performance benefit from using a reed valve instead of the current hardware for introducing EGR.

EGR Introduction: Combination Venturi and Reed Valve

The model was modified to have a venturi and a reed valve. This was run at AVL modes 4 and 8 and the results compared with the standard system with a venturi only. The addition of a reed valve increased the EGR rate by 5% (AVL mode 4) and 2.4% (AVL mode 8). IMEP and ISFC were unchanged. This suggests only a marginal benefit in EGR rate with the addition of a reed valve.

Effect of Modified EGR Venturi

The diffuser angle of the standard EGR venturi is 12 degrees. The GT-Power model was run at AVL mode 8 with a diffuser angle of 6 degrees. A gentler diffuser angle should improve pressure recovery downstream of the venturi and thereby improve engine performance by reducing inlet system pressure losses. However, the model predicted no change in engine IMEP and ISFC. EGR rate increased slightly from 16% to about 17%. In reality, a wide diffuser angle (12 degrees) is likely to suffer from flow separation at the wall and result in loss of pressure recovery. The GT-Power model is not designed to

handle this and so cannot predict a change in performance in this case. Computational fluid dynamics simulation or actual engine tests are required for further understanding.

The throat of the EGR venturi accelerates the gas flow, resulting in the low-pressure region necessary to draw EGR into the intake line. The GT-Power model was run at AVL mode 8 with its original venturi throat diameter and a diameter with nearly 55% less flow area. As hoped, with the smaller diameter the EGR rate increased, in this case from 16% to 23% (Figure 19).

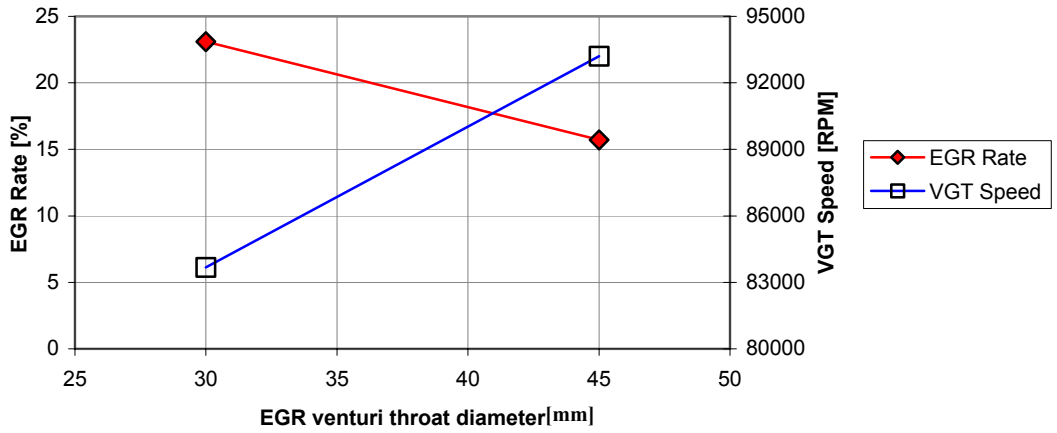

Figure 19: Effect of EGR Venturi Throat Diameter on EGR Rate and VGT Speed at AVL Mode 8

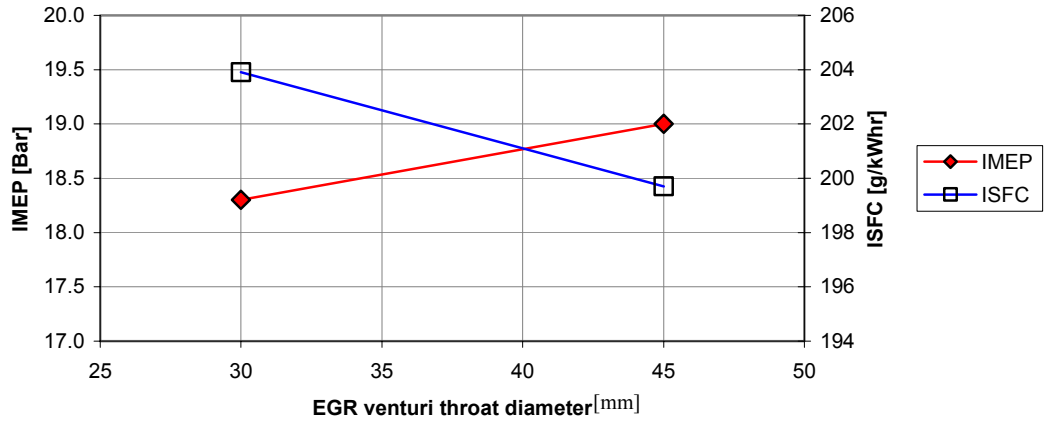

Figure 20: Effect of EGR Venturi Throat Diameter on IMEP and ISFC at AVL Mode 8

However, the smaller throat reduced the IMEP by 3% and increased the ISFC by 2% (Figure 20). Reducing the throat diameter will increase the EGR rate but with a performance penalty.

GT-Power: Summary of Potential Engine Modifications

The advantages and disadvantages of the modeled hardware changes are summarized in Table 1.

Table 1: Summary of Potential Engine Modifications

Potential Modification	Advantages	Disadvantages	Potential Option for Future?
Improve EGR distribution between cylinders	Optimizes NO_x reduction and improves engine performance	Performance—none, could impact engine package	Yes
Shorter heat release period at high-speed/high-load points	Improves fuel economy	None	Yes
Switch to a smaller compressor in VGT	Better surge margin	Ambient conditions—none, may impact off-ambient robustness	Yes
Close the VGT turbine rack or use smaller turbine	Helps drive high levels of EGR	Could lead to VGT over-speed at high-speed/high-load operation	Yes
Use a larger EGR valve	None detected	Less resolution at low lift	No
Use a reed valve to drive more EGR	Mechanically simple device	Not likely to provide high EGR levels at high-speed/high-load points	No
Use a reed valve in combination with a venturi to drive more EGR	No significant increase in EGR rate over a venturi	Increased complexity	No
Modify EGR venturi diffuser	Improves pressure recovery in the intake line	Limited space to install a longer diffuser	Yes
Modify EGR venturi throat	Improves suction leading to significantly more EGR	Fuel efficiency penalty	Yes

Method of Achieving Ultra-Low NO_x Emissions

Screening of various concepts to meet the 0.5g/bhp-hr NO_x target was carried out with the GT-Power and XPNOx models, and hardware changes were identified. A smaller turbocharger compressor will improve the compressor surge margin as the EGR rate is increased. Simulations were run at the AVL 8-mode points, producing target engine settings to achieve the 0.5g/bhp-hr NO_x target over the AVL 8-mode test. The effect on fuel efficiency was also estimated.

Figure 21 shows the effect if injection timing retard is required in addition to high EGR. The high EGR strategy reduces the NO_x to 0.5 g/bhp-hr with about a 2% efficiency penalty. An additional 5-degree retard reduces the NO_x to about 0.3 g/bhp-hr, but the efficiency penalty increases to 7%. Given validation experience, it is expected that the NO_x predictions are accurate within 10%-20%. A fuel consumption penalty of 4% is probably a realistic target at this stage.

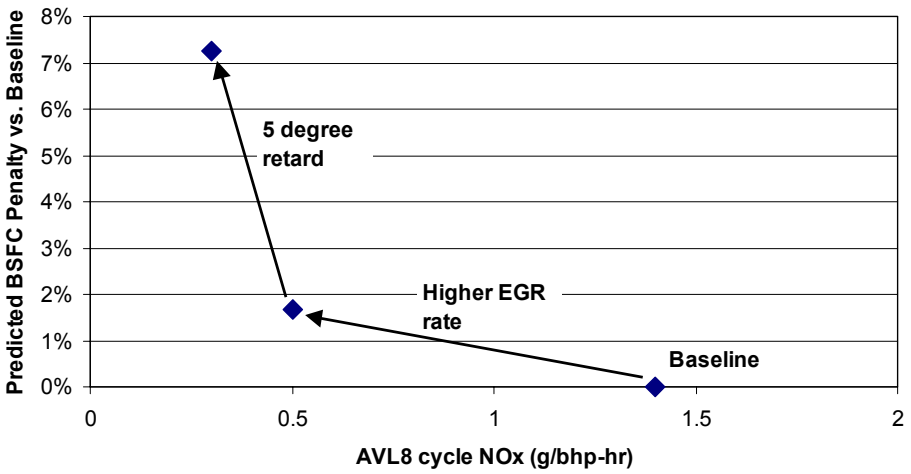

Figure 21: Impact of Injection Timing Retard on Fuel Efficiency Penalty

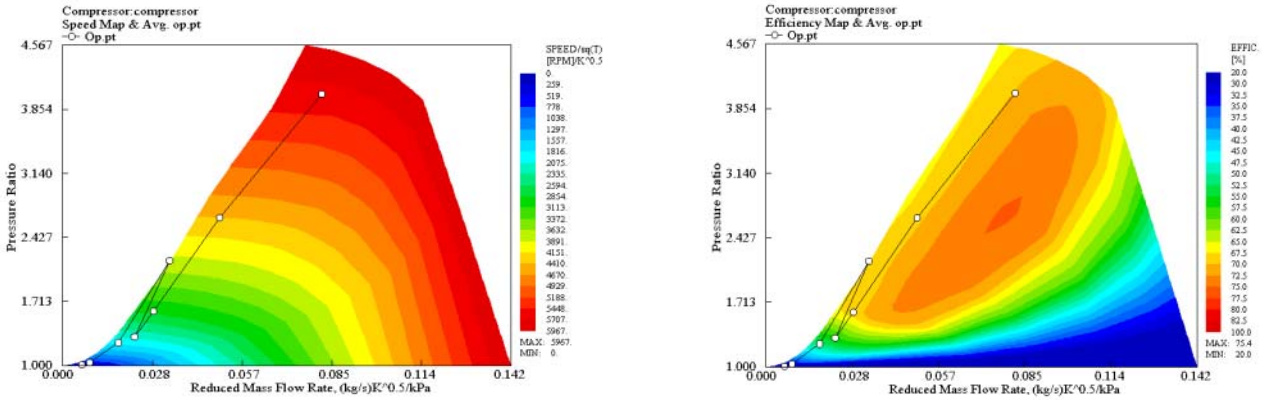

Figure 22: 0.5 g/bhp-hr NO_x Model of AVL Test Points on Smaller Trim Compressor Speed and Efficiency Maps

Figure 22 shows the AVL 8-mode operating points on the VGT compressor speed and efficiency maps. To avoid surge, the original compressor map was replaced with that of a smaller compressor. Even with this change, the 0.5-g NO_x recipe with higher EGR rates and reduced airflow rates pushes the operating points close to the surge line.

3.3 Diesel Baseline Testing

3.3.1 Objective

Baseline testing was conducted to establish the emissions and performance of the diesel engine with EGR and to check data repeatability. Tests were performed at operating points representative of the full engine map, with emphasis on those points that are most critical to NO_x production.

3.3.2 Accomplishment Summary

The engine was tested with diesel fueling and EGR over two standard test cycles using the standard calibration. The AVL 8-mode cycle-weighted NO_x emissions were 1.97 g/bhp-hr. The ESC 13-mode emissions were 2.28 g/bhp-hr. This was an early development calibration, and the results are not necessarily indicative of current production diesel ISX engines with EGR.

3.3.3 Accomplishment Details

AVL 8-Mode Test Cycle

The AVL 8-mode test is a steady-state test designed to correlate closely with the emission results from the Federal Test Procedure (FTP) heavy-duty transient test (Figure 6). The cycle-weighted NO_x emissions were 1.97 g/bhp-hr using the calibration provided. This was an early development calibration, and the results are not necessarily indicative of current production diesel ISX engines with EGR. Table 2 shows a mode-by-mode breakdown.

There were very low EGR rates at mode 4; this likely accounts for the high NO_x emissions at this mode. Early in the testing program, operating instabilities were encountered with the VGT and air handling system near this operating point. Hardware changes made later in the program removed any instabilities.

Table 2: AVL 8-Mode Test Results under Diesel Fueling

AVL Mode	Speed (rpm)	Load (%)	BSNOx (g/bhp-h)	BSnmHC (g/bhp-h)	BSCO (g/bhp-h)	BSCH4 (g/bhp-h)	Diesel BSFC (g/bhp-h)
2	732	25	3.31	0.25	0.74	0.00	190.6
3	854	63	3.28	0.10	0.24	0.00	165.9
4	984	84	5.81	0.07	0.12	0.00	165.9
5	1800	18	2.95	0.44	1.12	0.00	256.4
6	1740	40	1.30	0.24	0.79	0.00	191.9
7	1740	69	1.26	0.13	0.58	0.00	185.5
8	1668	95	1.30	0.07	0.34	0.00	180.5
Composite Results			**1.97**	**0.18**	**0.64**	**0.00**	**194.9**

ESC 13-Mode Test Cycle

The ESC is a steady-state test with 13 modes (Figure 23). It is used in the Supplemental Emissions Test as part of the EPA certification procedures for heavy-duty on-highway engines. The test points are uniformly distributed under the torque curve, making it a useful test for mapping the engine calibration.

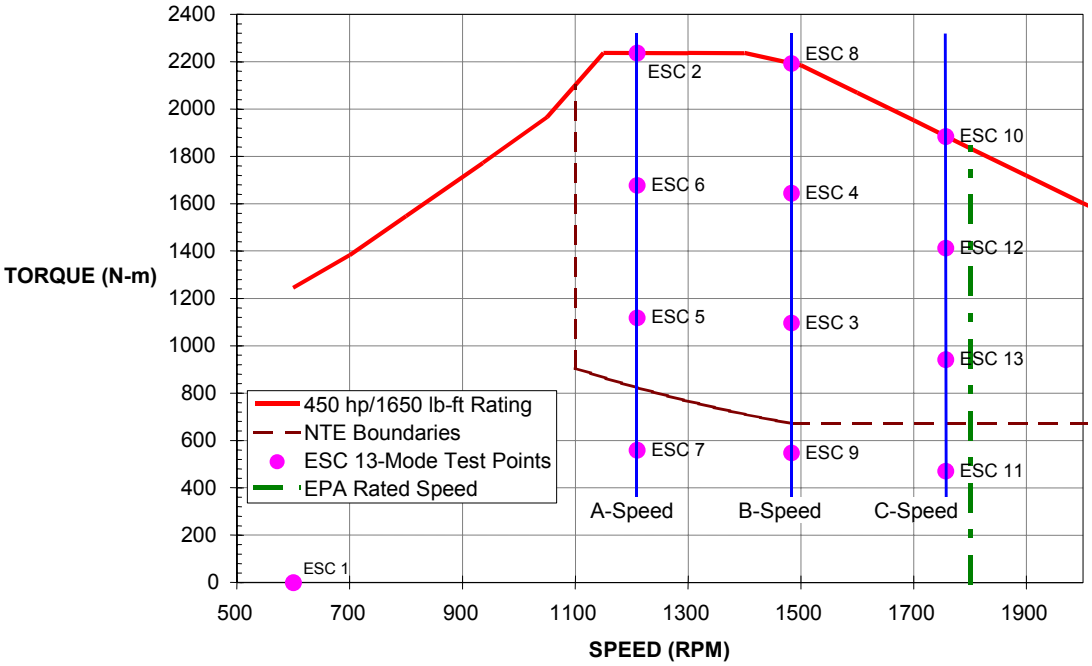

Figure 23: ESC 13-Mode Test Points and Torque Curve

The ESC cycle-weighted NO_x emissions were 2.28 g/bhp-hr with diesel fueling using the calibration provided. Like the AVL results, this was an early development calibration, so the results are not necessarily indicative of current production diesel ISX engines with EGR. Table 3 shows a mode-by-mode breakdown.

Table 3: ESC 13-Mode Test Results under Diesel Fueling

ESC Mode	Speed	Load (%)	BSNOx (g/bhp-h)	BSnmHC (g/bhp-h)	BSCO (g/bhp-h)	BSCH4 (g/bhp-h)	Diesel BSFC (g/bhp-h)
2*	A	100	1.40	0.06	1.24	0.00	160.2
3	B	50	2.22	0.09	0.42	0.00	165.4
4	B	75	2.23	0.06	0.43	0.00	155.2
5	A	50	3.34	0.08	0.69	0.00	156.1
6	A	75	2.01	0.05	0.58	0.00	155.1
7	A	25	3.81	0.16	0.42	0.00	168.5
8	B	100	1.76	0.04	0.47	0.00	159.2
9	B	25	2.85	0.14	0.49	0.00	184.2
10	C	100	1.88	0.05	1.03	0.00	157.1
11	C	25	4.02	0.19	0.41	0.00	214.2
12	C	75	1.93	0.06	0.86	0.00	159.6
13	C	50	3.37	0.11	0.29	0.00	173.2
Composite Results			**2.28**	**0.07**	**0.69**	**0.00**	**162.8**
	* Note: At mode 2 maximum torque reached 88% instead of 100%						

3.4 HPDI Baseline Testing

3.4.1 Objective

The diesel fuel system hardware was replaced with the HPDI fuel system for natural gas fueling. Baseline testing was conducted to determine the initial performance and emissions of the HPDI engine with EGR and to confirm functionality of the HPDI fuel system with EGR.

3.4.2 Accomplishment Summary

The HPDI fuel system was installed on the engine, and an initial calibration was developed using basic timing and EGR rate swings. The engine was tested over the AVL 8-mode test with the original J-31 injectors and a constant fuel pressure of 23 MPa. The cycle-weighted results were 1.46 g/bhp-hr for NO_x with a 177.6 g/bhp-hr diesel-equivalent fuel consumption. These tests were conducted early in the development program and are not necessarily optimal.

The J-31 injectors were replaced with newer J-34 injectors, and three injector tips with different nozzle geometries were tested. An injector tip using an 18-degree, 0.72-mm diameter nozzle geometry was selected as the most suitable of the three.

3.4.3 Accomplishment Details

HPDI Hardware Conversion

The production diesel fuel system was removed from the engine and replaced with a pre-production HPDI fuel system, including the following:

- An integrated fuel supply module (IFSM) that regulates high-pressure diesel and natural gas and delivers them to the fueling rails in the head
- A fuel pump for delivering high-pressure diesel to the IFSM
- J-31 HPDI fuel injectors, which are solenoid actuated
- An intelligent driver module (IDM), which includes the electronic controls for the HPDI system
- The necessary wiring harnesses

The IFSM (Figure 24) is situated on the air inlet side of the head. The high-pressure diesel is manually regulated from 15-25 MPa. The natural gas pressure is regulated by the dome-loaded self-relieving regulator to a pressure slightly lower than the diesel pressure, to ensure that no natural gas leaks into the diesel side of the injector. Diesel is supplied to the IFSM by a high-pressure fuel pump driven from the engine crankshaft (Figure 25).

Figure 24: Photograph of the IFSM Assembly

Figure 25: High-Pressure Diesel Fuel Pump

The stock diesel fuel injectors, which are actuated by a cam and rockers, were removed along with the valve rocker assembly, and the J-31 HPDI fuel injectors (Figure 26) were installed (Figure 27).

Figure 26: The J-31 HPDI Injector

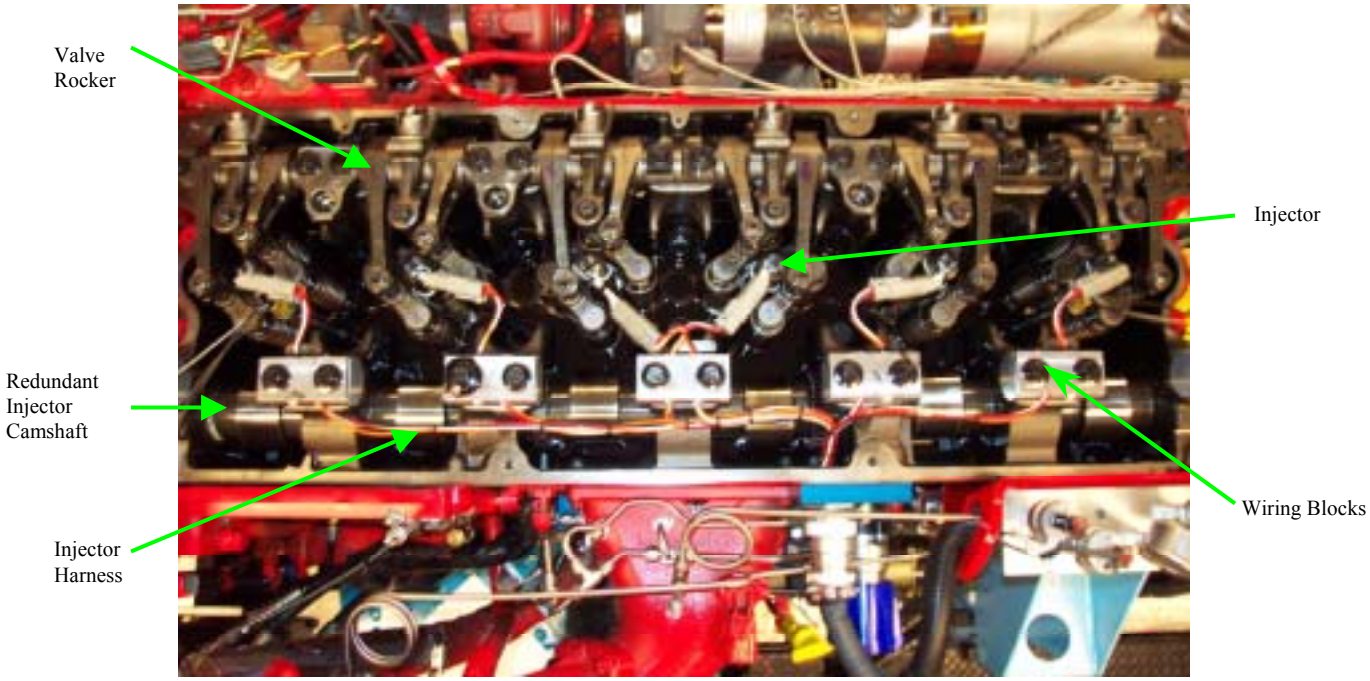

Figure 27: Installed J-31 Injectors and Wiring Harness

The control architecture is incremental, meaning the existing Cummins CM870 ECM drives an added Westport IDM, which further modifies some of the output signals. Figure 28 shows the signals that the injector receives from the Westport IDM controller.

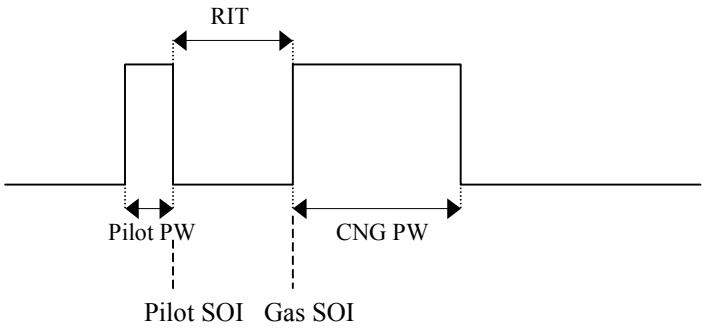

Figure 28: Injection Pulse and Timing Diagram

Inherent in any "common rail" type injector with electro-hydraulic actuation is a delay between commanded timing and actual fuel delivery. The timing offset can be used to compensate for injection delay or differences in injection rate shape between the baseline diesel and gas engines.

Preliminary HPDI Calibration: AVL 8-Mode Test Cycle

After installation of the HPDI fuel system, the engine was recalibrated for initial operation. Basic timing and EGR swings were conducted at all AVL and some ESC modes to give good coverage of the engine speed and load range. New timing and EGR fraction maps were determined from the tradeoff between fuel consumption and NO_x emissions, with the carbon monoxide (CO) emissions also monitored to ensure that they were not excessive. Fuel pressure was maintained at 23 MPa. The resulting HPDI calibration had slightly higher EGR rates than the diesel calibration. The resulting AVL 8-mode weighted NO_x emissions were 1.46 g/bhp-hr. A breakdown of the AVL 8-mode test results is given in Table 4.

Table 4: AVL 8-Mode Test Results under HPDI Fueling with Initial Calibration

AVL Mode	Speed (rpm)	Load (%)	Measured EGR Fraction (%)	BSNOx (g/bhp-h)	BSnmHC (g/bhp-h)	BSCO (g/bhp-h)	BSCH4 (g/bhp-h)	Diesel Equivalent BSFC (g/bhp-h)
2	732	25	27.2	4.16	0.20	1.98	1.80	172.6
3	854	63	22.3	2.14	0.09	1.20	0.61	151.0
4	984	84	8.1	3.22	0.05	0.91	0.22	145.3
5	1800	18	30.1	2.55	0.29	2.99	4.29	248.2
6	1740	40	30.0	0.99	0.16	2.03	2.58	180.2
7	1740	69	23.6	0.77	0.07	1.11	1.28	169.2
8	1668	95	15.0	0.80	0.06	1.21	0.55	173.0
Composite Results			--	**1.46**	**0.11**	**1.52**	**1.46**	**177.6**

This initial testing showed that at low speed and load conditions, NO_x emissions are reduced as the gas rail pressure (GRP) is reduced, so fuel pressure becomes a variable in later tests.

Injector Upgrade

After initial testing with J-31 injectors, newer J-34 HPDI fuel injectors became available, so the engine was upgraded to these. Improvements in the J-34 include the following:

- Improved design for manufacture
- Increased injection pressure capability
- Better pilot injection flexibility

The increased injection pressure capability allows a faster injection rate, especially at high speed and high load, where the heat release period is critical in diesel-cycle engines. The tables in the Westport controller were modified to suit the characteristics of the J-34 injectors.

Nozzle Geometry Selection

The match between the injector nozzle geometry and the combustion system (combustion bowl, in-cylinder air motion, and ignition source) is critical in any late-cycle, direct injection engine (HPDI, diesel, and gasoline direct injection). Therefore, three different HPDI nozzle configurations were tested and evaluated.

Results from earlier non-EGR ISX test programs showed that a 15-degree nozzle matches this combustion system, so two sets of nozzles were configured with a 15-degree angle. Each set had a different jet hole diameter (0.72 mm and 0.77 mm were tested), giving a difference in injection rate and jet penetration, the typical distance traveled by the fuel jet into the cylinder. Injectors of 18 degrees were also tested with holes of 0.72 mm—these gave the best overall results, so all future work used this configuration.

3.5 Preliminary Optimization: EGR Rate, Injection Timing, Fuel Pressure

3.5.1 Objective

Initial performance and emissions optimization was conducted by varying the EGR rate, injection timing, and fuel pressure. The relationship between these parameters and engine performance and emissions was examined to determine areas where further optimization and refinements are most needed.

3.5.2 Accomplishment Summary

EGR rates were varied from approximately 8%-30% at constant fuel pressure and injection timing. As expected, NO_x emissions decreased as EGR rates increased but with CO and BSFC penalties. At high loads, NO_x was not reduced as much as desired for the program goals.

Pilot timing and quantity was varied at ESC mode 3 using a constant fuel pressure of 23 MPa. In general, as the pilot quantity decreased and the relative injection timing (RIT) increased, the combustion of the main gas charge became more erratic. This poor gas combustion adversely affects emissions and fuel consumption. Pilot injection quantities of 5-10 mg per injection provide the best tradeoff of emissions and efficiency without adversely affecting combustion.

GRP was varied from 23-28 MPa at high loads and speeds. The presence of EGR slows the rate of combustion. The increased fuel injection rate resulting from higher fuel pressures increases the rate of combustion. Therefore, as EGR rates increase at higher speeds and loads, the fuel pressure may be increased to control the rate of combustion.

3.5.3 Accomplishment Details

EGR Swings

A five-point EGR swing was conducted with constant fuel pressure and injection timing while the gas pulse width controlled the engine torque. The EGR rate was swung up to +/- 25% of the nominal EGR rate from the diesel-fueled ECM map. As expected, NO_x emissions decreased as EGR rate increased, with some BSFC and CO penalties. The CO

level is an important indicator of combustion quality and onset of incomplete combustion, with considerable CO increases taken as an indication of incomplete combustion. Figure 29 shows these responses at ESC modes 5 and 10.

At mode 5, one of the more difficult not-to-exceed (NTE) conditions at which to achieve low NO_x, the NO_x versus BSFC tradeoff experienced a 5.4% increase in BSFC for a 75% reduction in brake specific NO_x ($BSNO_x$) by application of up to 30% EGR. The minimum NO_x level achieved was 0.5 g/bhp-hr, well below the 0.75g/bhp-hr limit required to meet NTE requirements for a 0.5g/bhp-hr engine (based on an NTE factor of 1.5, required for engines with NO_x Family Emission Limits below 1.5g/bhp-hr).

Figure 29 also shows the EGR swing data at ESC mode 10. Here the EGR valve is generally fully open, and the only way to increase the EGR rate is to increase the pressure differential across the EGR system by closing the VGT, increasing the backpressure in the exhaust manifold in relation to the boost pressure in the inlet manifold.

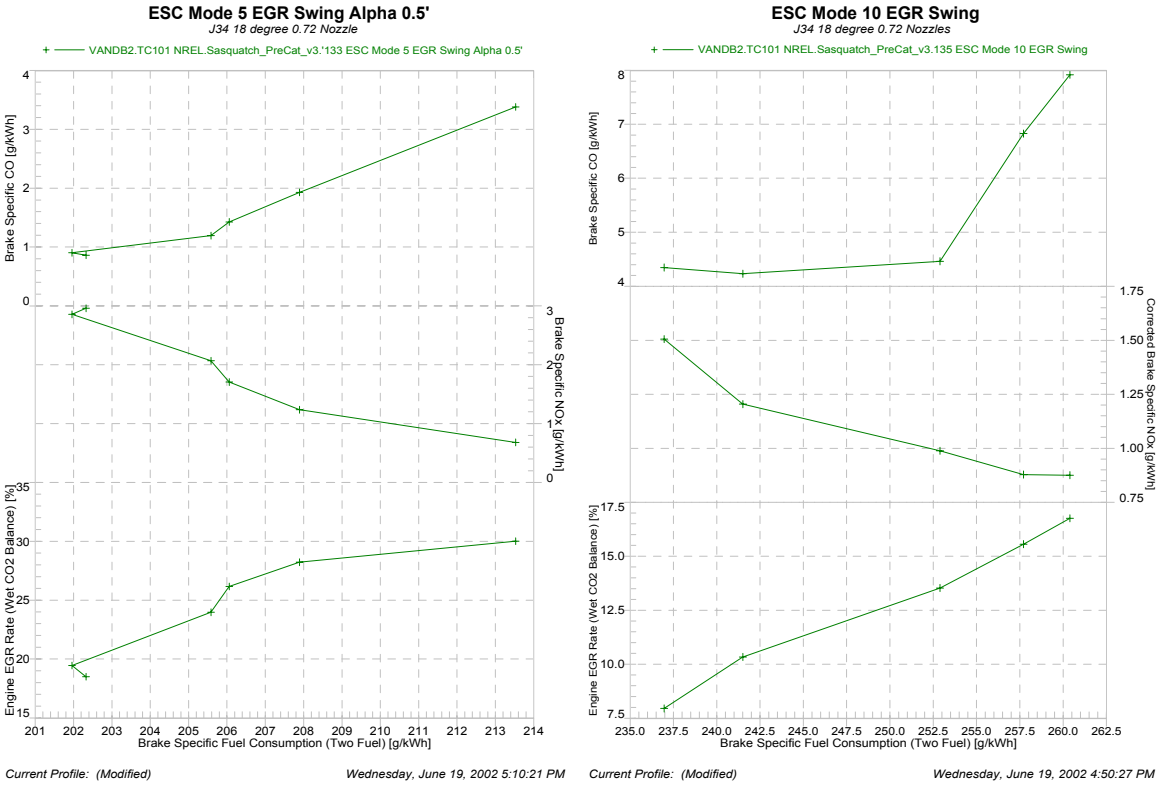

Figure 29: ESC Mode 5 and 10 EGR Swings

The NO_x versus BSFC tradeoff shows that for a 9% increase in BSFC the $BSNO_x$ was reduced by 40% to a minimum level of 0.65g/bhp-hr, close to the target of 0.5g/bhp-hr. The efficiency here was disappointing, and a significant improvement was required to meet the program goals.

Pilot Fueling Swings

Pilot timing and quantity were varied with the objective of minimizing pilot fuel consumption while maintaining good combustion and emissions. Pilot pulse width (PPW) and RIT, the delay between the pilot and gas injection, were varied at ESC mode 3 using

a constant fuel pressure of 23 MPa. This test mode (1,498 rpm and 50% load) is close to on-highway cruise conditions and an important contributor to methane (CH_4) emissions on an ESC test.

EGR rate was kept constant at 30% +/- 1%, and the start of gas injection was kept constant. The gas pulse width was adjusted to maintain a constant torque. The start of combustion was allowed to vary as the PPW and RIT changed. Typically, start of combustion was between top dead center and 5 degrees ATDC.

The tests indicated that pilot injection quantities of 5-10 mg per injection provided the best tradeoff of emissions and efficiency without adversely affecting combustion. Similar tests may be conducted in the future at other operating points.

In general, as the pilot quantity decreases and the RIT increases, the combustion of the main gas charge becomes more erratic. This poor gas combustion adversely affects emissions and fuel consumption. A summary of the results is shown in Table 5, and the performance responses are shown graphically in Figure 30 through Figure 34.

For this application and emissions level, a pilot quantity of 5-10 mg per injection is preferred because of the low $BSNO_x$, BSFC, and pilot energy ratio. This information will assist in range setting during the later multivariable optimization phase.

Table 5: Summary of Pilot Fueling Swings

Pilot Quantity Range	Positive Impact	Negative Impact	Select/Deselect
0-5 mg/inj	• Pilot energy ratio < 5%	• COV of IMEP up to 5% • High CH_4 • Large sensitivity to pilot timing	**Deselect**—combustion is marginal and close to misfire
5-10 mg/inj	• Best NO_x vs. BSFC trade off • COV of IMEP < 2% • Low NO_x • Low BSFC • Pilot energy ratio < 8%	• Higher pilot energy ratio • CH_4 variability	Select for low-NO_x applications where CH_4 regulations allow
10-15 mg/inj	• Best BSFC • Low CH_4 • Low CH_4 sensitivity to timing • Low CO potential • Good NO_x vs. BSFC	• Pilot energy ratio up to 11%	Select when CH_4 and CO are critical and NO_x levels can be higher
15-20 mg/inj	• Lowest COV of IMEP • Low CO potential • Lowest CH_4 • Low CH_4 sensitivity to timing • Good BSFC	• Poor NO_x vs. BSFC • High CO sensitivity • Pilot energy ratio up to 15%	**Deselect**—pilot energy ratio and NO_x are high

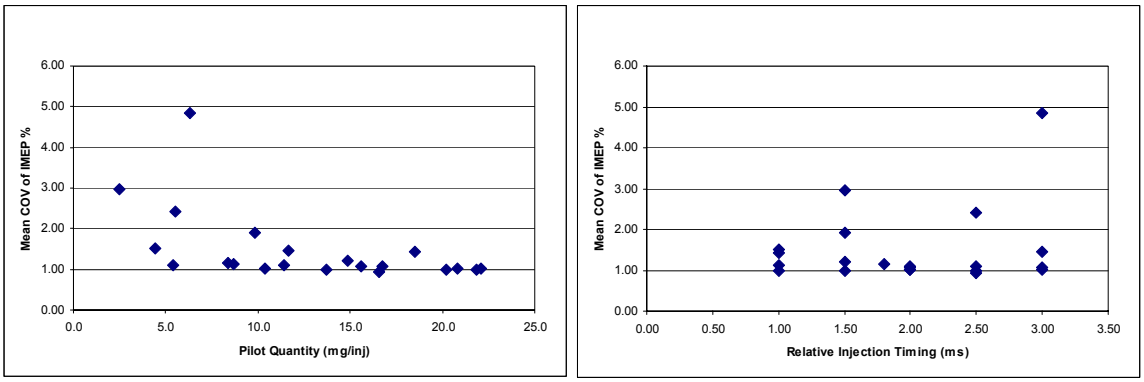

Figure 30: Pilot Fueling Swings—Coefficient of Variance (COV) of IMEP Response

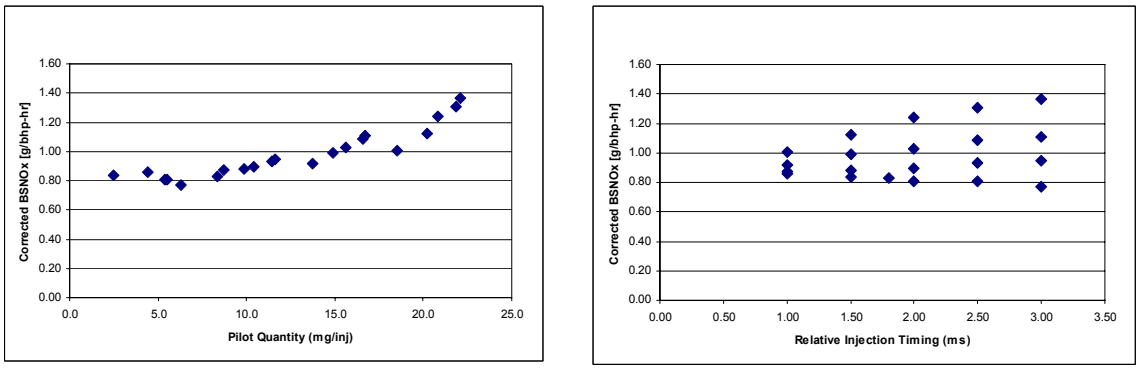

Figure 31: Pilot Fueling Swings—Corrected $BSNO_x$ Response

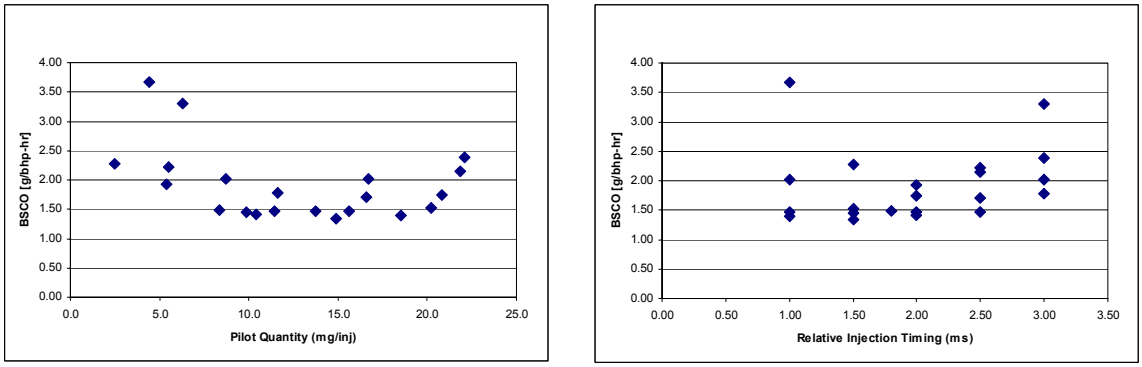

Figure 32: Pilot Fueling Swings—Brake Specific Carbon Monoxide (BSCO) Response

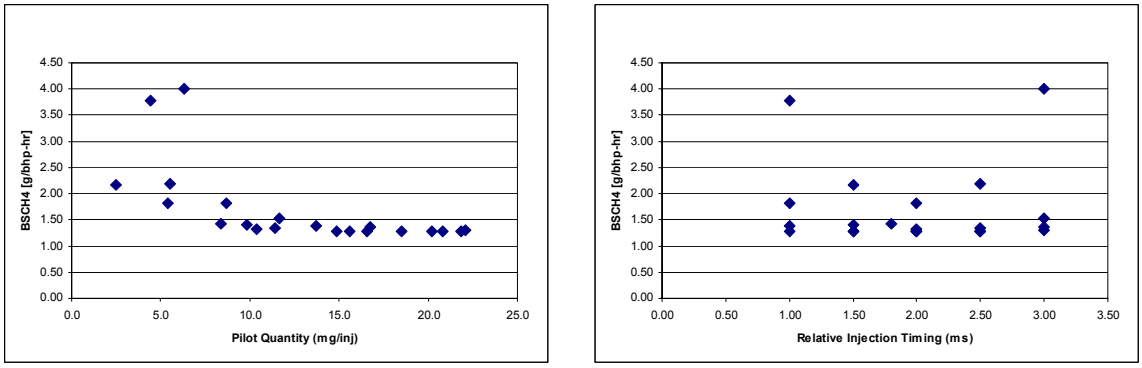

Figure 33: Pilot Fueling Swings—Brake Specific CH_4 ($BSCH_4$) Response

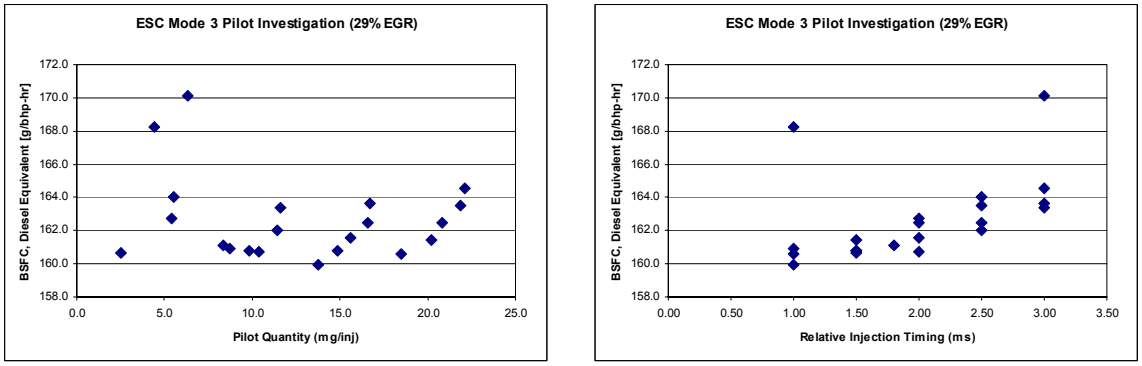

Figure 34: Pilot Fueling Swings—BSFC Response

GRP Swings

High EGR rates are necessary for low NO_x emissions at high loads, but the heat release period increases, resulting in poorer efficiency. Increasing the gas injection pressure, which increases the injection rate, shortens the heat release again.

Tests were conducted at GRPs of 23, 25, and 28 MPa at AVL mode 8 (100% load at 1,668 rpm) and ESC mode 10 (100% load at 1,757 rpm). The EGR rate was held constant at 21% and 16% for the AVL mode 8 and ESC mode 10 tests, respectively.

The results at AVL mode 8 are shown in Figure 35 through Figure 38. Operation at 23 MPa was limited because retarding the timing resulted in the exhaust gas temperature (EGT) exceeding its limit, whereas advancing the timing resulted in exceeding the maximum allowable cylinder pressure.

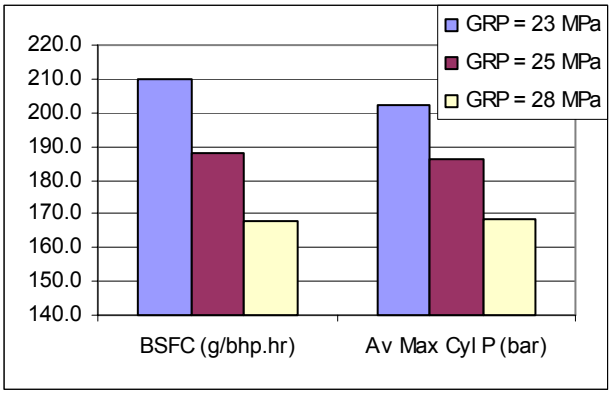

Figure 35: AVL Mode 8 GRP Swings—BSFC and maximum cylinder pressure (Pmax).

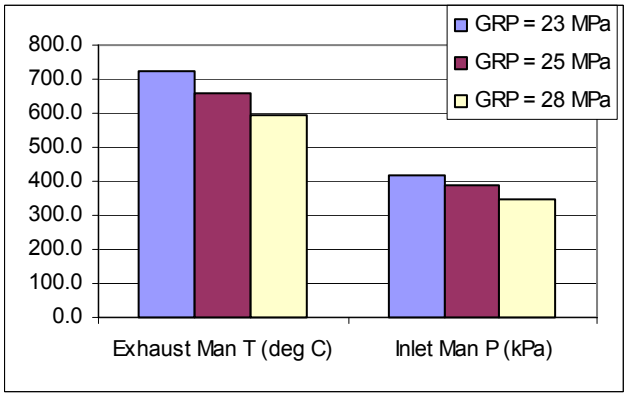

Figure 36: AVL Mode 8 GRP Swings—EMT and IMP

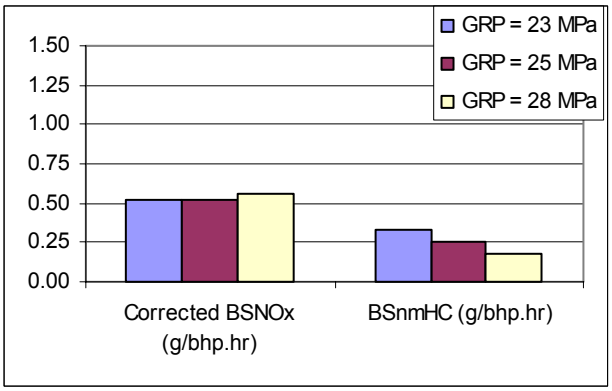

Figure 37: AVL Mode 8 GRP Swings—$BSNO_x$ and BSNMHC

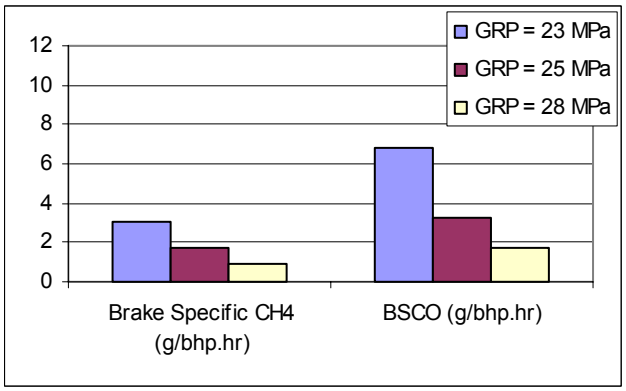

Figure 38: AVL Mode 8 GRP Swings—$BSCH_4$ and BSCO

The results of the gas pressure swings at ESC mode 10 are shown in Figure 39 through Figure 42. At these high load and speed conditions, high injection pressures give better efficiency. At AVL mode 8, BSFC dropped by about 20% as GRP increased from 23 to 28 MPa. At ESC mode 10, BSFC dropped by about 8.5%. NO_x increased slightly but remained within reasonable limits. Further optimization is expected to reduce these NO_x levels. The higher injection pressures also resulted in reduced emissions of all other regulated pollutants.

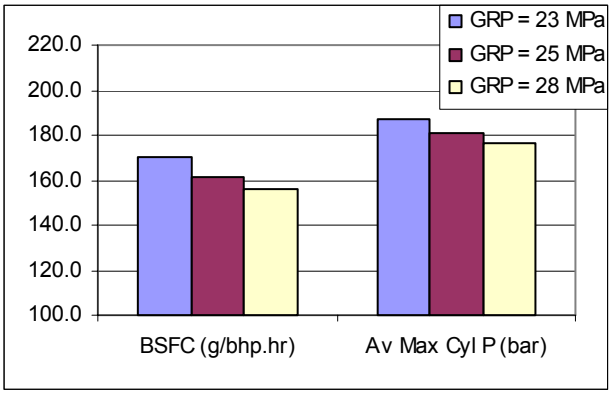

Figure 39: ESC Mode 10 GRP Swings—BSFC and Pmax

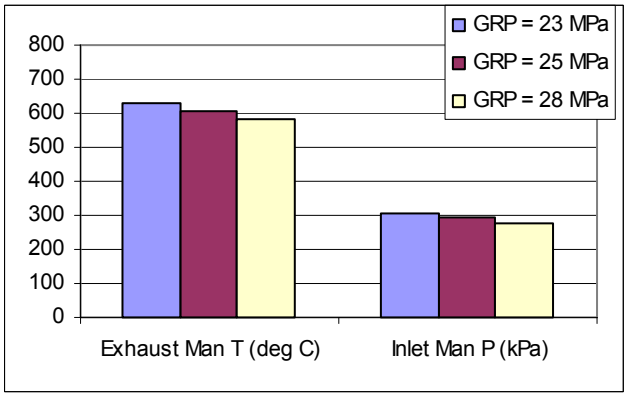

Figure 40: ESC Mode 10 GRP Swings—EMT and IMP

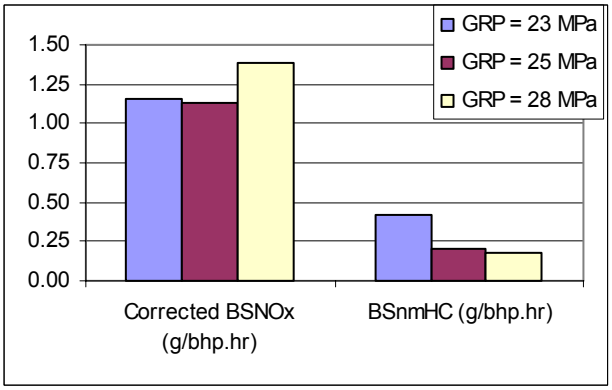

Figure 41: ESC Mode 10 GRP Swings—$BSNO_x$ and BSNMHC

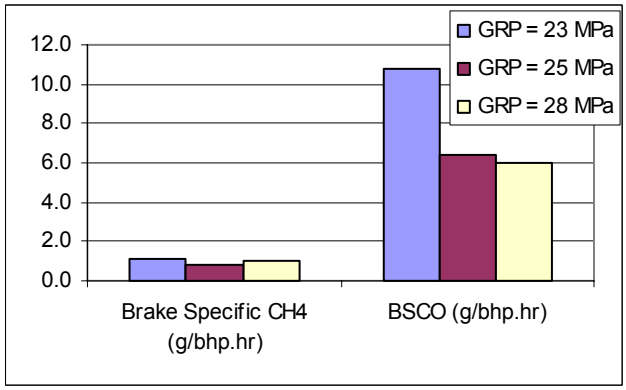

Figure 42: ESC Mode 10 GRP Swings—$BSCH_4$ and BSCO

In general, increasing the injection pressure shortens the heat release period, giving a more efficient gas expansion and less heat lost to the exhaust, seen as lower exhaust temperatures (Figure 36 and Figure 40). Less heat through the exhaust results in less energy to the turbocharger and therefore a lower intake manifold pressure (Figure 36 and Figure 40). This results in lower peak cylinder pressures (Figure 35 and Figure 39). In short, higher injection pressure is beneficial for emissions, efficiency, and engine durability.

3.6 Oxidation Catalyst Testing

3.6.1 Objective

Oxidation catalysts were sourced and tested with the following objectives:

- Obtain several oxidation catalysts based on preliminary emissions results and compare their PM conversion efficiencies
- Determine the PM breakdown of solid material and soluble organic fraction (SOF)
- Select an optimal oxidation catalyst formulation and determine the effect of the selected catalyst size and formulation on gaseous and PM emissions

3.6.2 Accomplishment Summary

Three oxidation catalysts were selected and sourced from two suppliers, NET and Engelhard. These were tested at varying EGTs and space velocities. PM measurements were taken without a catalyst for analysis of volatile/non-volatile content. PM measurements were taken before and after a combination of oxidation catalysts to determine PM conversion efficiency. AVL 8-mode PM emissions were reduced by 34% from 0.04 g/bhp-hr to 0.03 g/bhp-hr. Nonmethane hydrocarbon (NMHC) emissions were reduced by 54% and CO emissions by 96%. The relatively poor NMHC conversion suggests high quantities of ethane or propane in the exhaust. The natural gas fuel composition for these tests was typical "line gas," which contains approximately 96%-97% CH_4, less than 2% ethane, less than 0.5% propane, and less than 1% inert gases on a molar fraction basis.

3.6.3 Accomplishment Details

Catalyst Comparison

The objective of adding an oxidation catalyst to the HPDI EGR engine is to reduce NMHC, CO, and PM levels. Three oxidation catalysts with different precious metal loadings were sourced and tested to characterize their conversion efficiencies and to select the most appropriate catalyst size and formulation. The catalysts were as follows:

- 40 g/ft^3 precious metal loading (100% Pt) from NET
- 80 g/ft^3 precious metal loading (50% Pt and 50% Pd) from Engelhard
- 160 g/ft^3 precious metal loading (50% Pt and 50%Pd) from Engelhard

These precious metal loadings are higher than in current heavy-duty diesel applications, where catalyst activity is limited by fuel sulfur content and the resulting production of sulfate-based PM. With HPDI, this concern is eliminated by the ultra-low sulfur content of natural gas. All three catalysts had 9.5-in diameters and were 6 in long (approximately 7 L).

The engine used J-34 injectors operating with a GRP of 28 MPa and the following test matrix:

- Space velocity (SV) = 50,000 hr^{-1} at pre-catalyst EGT = 200°C, 250°C, 300°C, 350°C
- SV = 100,000 hr^{-1} at pre-catalyst EGT = 200°C, 250°C, 300°C, 350°C, 400°C
- SV = 150,000 hr^{-1} at pre-catalyst EGT = 275°C, 300°C, 350°C, 400°C, 425°C

Results are shown in Figure 43, Figure 44, and Figure 45. CO conversions were similar for all three catalysts: over 90% at SV = 50,000 and 100,000 and over 85% at SV = 150,000. An upper limit of approximately 95% conversion efficiency was achieved at EGT > 200°C and SV = 50,000. The light-off temperature of CO is less than 200°C and is expected to be around 150°C.

As expected, CH_4 conversion efficiency was very low, less than 15% at all conditions. For the 40-g/ft^3 catalyst, loaded lightly with Pt, there was only a slight rise in CH_4

conversion as EGT rose (Figure 43). Given an error estimate of +/- 5%, there was no clear effect of SV on conversion efficiency. This is not surprising because the conversion efficiency under the chemical kinetic rate limit is highly dependent on temperature, not mass flow. A maximum CH_4 conversion efficiency of 10% was seen at EGT > 400°C with SV = 150,000 and EGT > 350°C with SV = 50,000. Increasing the size of the catalyst under these conditions will have little effect on the conversion efficiency.

With the addition of 40 g/ft^3 Pd to the catalyst, slightly higher conversion efficiencies were achieved (Figure 44). For example, peak CH_4 conversions of 13% were realized with 40 g Pt and 40 g Pd, versus 10% with 40 g Pt (ignoring any effects of the washcoat). However, there was still little effect on the conversion efficiencies when SV was varied from 50,000 to 150,000. This confirms that chemical kinetics are rate-limiting under the relatively low EGTs.

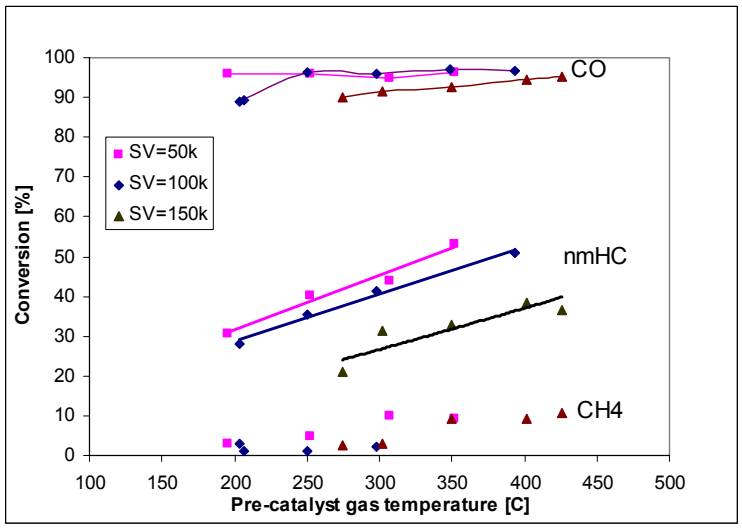

Figure 43: CO, NMHC, and CH_4 Conversion Efficiencies of 40 g/ft^3 Catalyst

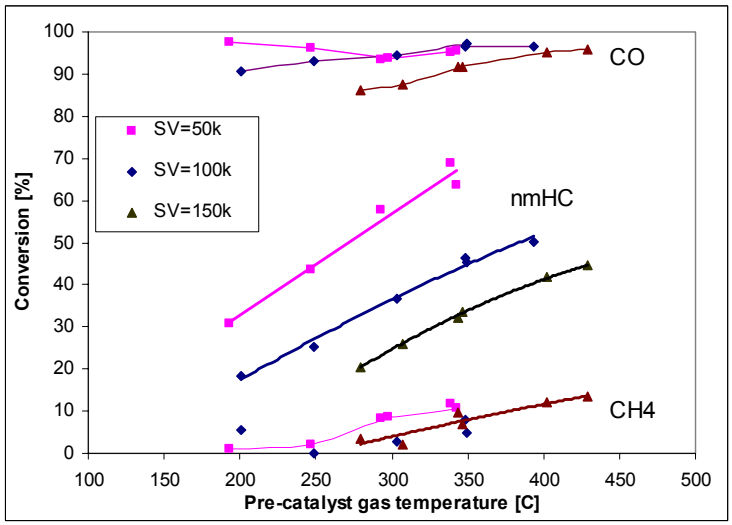

Figure 44: CO, NMHC, and CH_4 Conversion Efficiencies of 80 g/ft^3 Catalyst

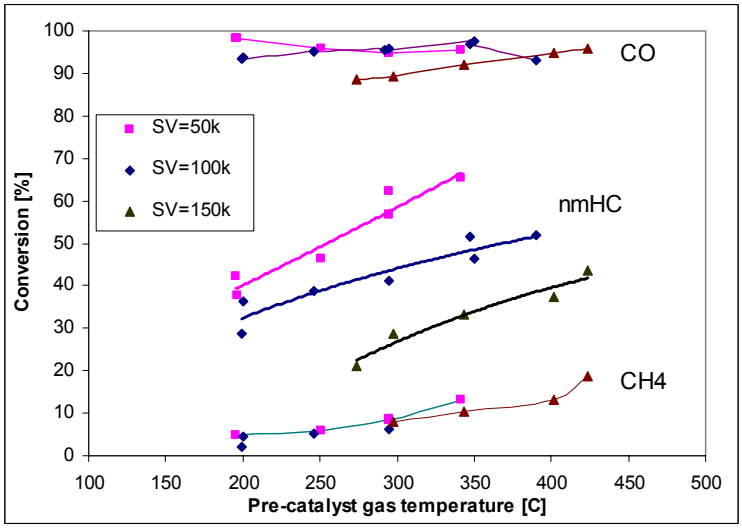

Figure 45: CO, NMHC, and CH_4 Conversion Efficiencies of 160 g/ft^3 Catalyst

Increasing the precious metal loading to 80 g Pt and 80 g Pd had a significant effect on the low-temperature CH_4 conversion efficiencies (Figure 45). The conversion efficiency at SV = 150,000 and EGT = 425°C was close to 20%, and at SV = 50,000 and EGT = 300°C was 13% (compared to 13% and 11%, respectively, for medium loading). The curve at SV = 150k appears to be near the light-off point for CH_4 conversion. Assuming a typical S-shaped curve, a small increase in the EGT would increase CH_4 conversion significantly. The trend suggests the light-off temperature at SV = 150,000 is approximately 450°C.

The light-off temperature is expected to be lower at lower space velocities. Once the chemical kinetics are no longer the rate-limiting factor, residence time becomes significant. Based on the above results, chemical kinetics may no longer be the rate-limiting factor at 350-400°C. At best, a light-off temperature of 400°C can be expected at very low catalyst space velocities.

The results from all catalysts suggest that the NMHC conversion efficiency is dependent on the SV, particularly when the SV is increased above 100,000. There is a slower increase in overall conversion efficiency with EGT at high SV compared with low SV.

The dependence of conversion efficiency on SV suggests that diffusion processes (pore or bulk) have begun to limit the conversion efficiency. However, given the complexity of the multi-component NMHC mixture (i.e., significantly higher light-off for major components propane and ethane), chemical rate limits for propane and ethane conversion and diffusion rate limits for heavy hydrocarbon components are expected. The majority of the converted species at the lower temperatures (< 300°C) is probably the heavier hydrocarbon fraction. The propane and ethane would only oxidize at the higher temperatures (> 300°C).

The results indicate that for control of NMHC a combined Pt/Pd catalyst is required. Space velocities should be moderate for the best control of NMHC. The recommended formulation and catalyst size were determined using simulation based on these results.

PM Breakdown

PM measurements were taken and the SOF analyzed. The engine was operating with J-34 injectors at 23 MPa GRP and calibrated to a 1.4 g/bhp-hr AVL NO_x level. The modal contributions of the PM over an AVL 8-mode test were examined.

The modal PM contribution to the composite AVL 8-mode result is shown in Figure 46. At each mode, the PM was broken down as SOF and solids. The solid content includes carbonaceous ash and sulfates. The SOF was further broken down as fuel or oil.

Overall, the SOF accounted for 38% (weighted basis) of the total PM. Of this, 40% was from a fuel-derived source, and 60% was from an oil-derived source. Modal SOF ranged from 24%-60%. Only modes 7 and 8, high load and speed, had SOF content below 50%. The results indicate that an oxidation catalyst is likely to reduce PM emission by around 30%. The actual value was established by pre/post catalyst tests.

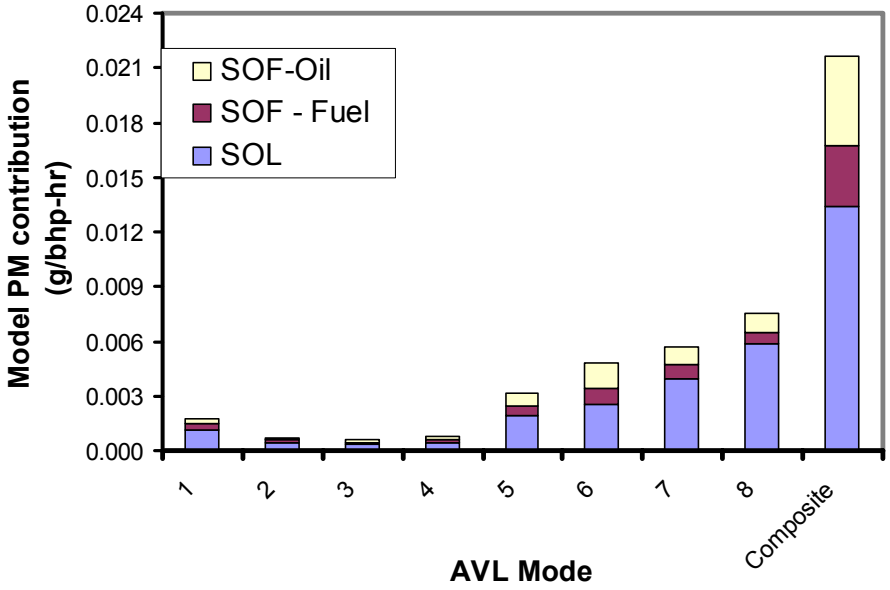

Figure 46: PM Modal Contribution Breakdown over AVL 8-Mode Test Cycle

AVL 8-Mode Test Results with Catalyst

The engine was tested on the AVL 8-mode test, resulting in 0.8 g/bhp-hr NO_x. It was fitted with 80 g/ft^3 and 160 g/ft^3 catalyst bricks with 50% platinum and 50% palladium. The total catalyst volume was 14 L. Gaseous emissions were sampled upstream and downstream of the catalyst. PM emissions were measured with a mini-dilution tunnel. The test was run twice, with PM first measured before the catalyst and second after the catalyst. Figure 47 shows that PM was reduced from 0.042 g/bhp-hr to 0.027 g/bhp-hr. NMHC emissions were reduced to 0.21 g/bhp-hr and CO emissions to 0.13 g/bhp-hr. As expected, no significant NO_x conversion was detected.

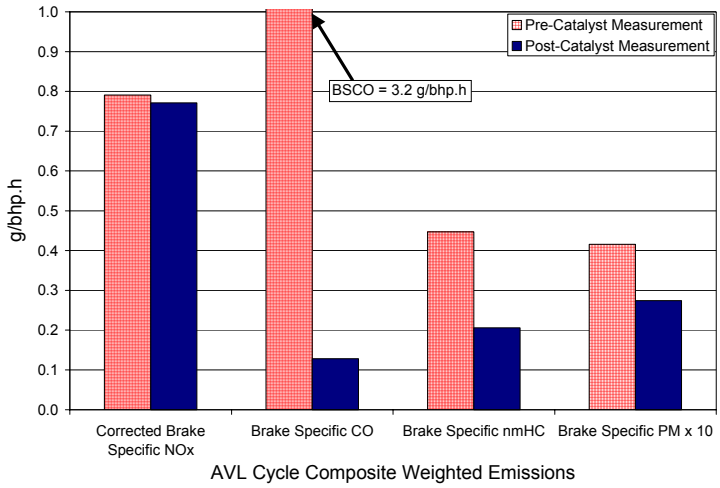

Figure 47: Comparison of AVL Cycle-Weighted Emissions Before and After Oxidation Catalyst

The conversion efficiencies for PM, NMHC, and CO (Figure 48) were within the ranges expected based on screening tests. In particular, the PM conversion efficiency was close to the SOF measured earlier. Although the catalyst activity was high, the conversion efficiency of NMHC was relatively low. This probably indicates a high ethane content in the NMHC.

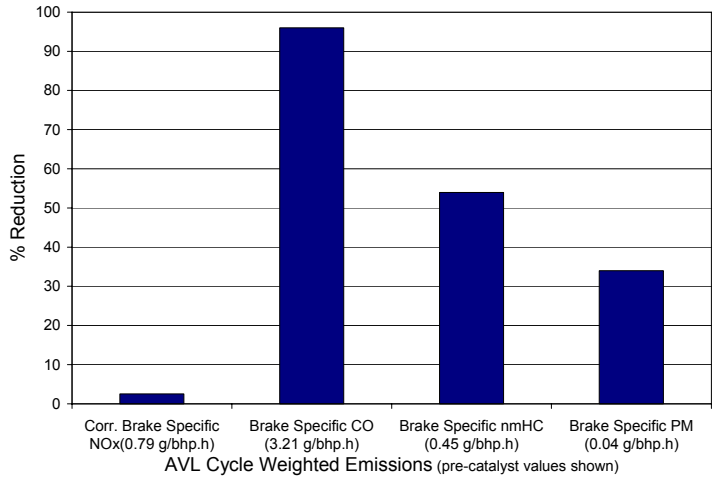

Figure 48: Emissions Reduction Resulting from Oxidation Catalyst (Based on AVL Weighted Emissions; See Figure 47)

3.7 Hardware and Controls Improvement

3.7.1 Objective

Modeling and testing indicated that engine hardware must change to achieve the emissions targets. The engine hardware was upgraded as necessary to meet the performance and emissions targets.

3.7.2 Accomplishment Summary

The engine was replaced with a production ISX 2002 engine and the latest production-intent HPDI fuel system hardware and controls. There were no fundamental differences between the tested development engine and the production engine.

The base engine and Westport controls were integrated. The engine was fitted with the revised turbocharger used on the previous engine. The new engine was tested on the AVL 8-mode test under manual control. The response of the new engine was very similar to the old engine, so all previous calibration work was directly transferable to this engine.

The engine was instrumented for measuring the EGR fraction. The EGR distribution within the head was examined at different speeds and loads. Less EGR was supplied near cylinders 6 and 5. This testing also identified the best sampling location and technique.

After the new engine was validated, a second EGR cooler was installed in series with the first. A 10%-30% reduction in AVL 8-mode NO_x is possible with additional EGR cooling applied at high speeds and loads. Coolant to the second cooler was initially provided by an independent water supply but was later routed from the engine coolant supply to prevent overcooling of the EGR.

3.7.3 Accomplishment Details

New Engine Installation and Validation

The new engine was a production ISX 2002 with the Westport production-intent prototype fuel system (Figure 49 and Figure 50). The base engine differed slightly from the previous development engine. The most significant change was a venturi flow meter that measures the EGR flow before it mixes with fresh air. This meter provided better feedback for the charge handling controls.

The main components of the production-intent Westport fuel system are an IFSM, a variable injection pressure (VIP) fuel pump, HPDI injectors, and a fuel control system. The new fuel supply module has a simpler design for manufacturing. It is attached to the head at the left side under the air intake (Figure 50). The VIP diesel pump is smaller than the previous pump and belt driven at the front of the engine.

The HPDI injectors were not changed. The J-34 type injector was used for the remainder of the project. Newer J-36 injectors, which are better designed for manufacturing, were entering production, but the calibration work on these was not complete. The J-34 injectors will be replaced by the J-36 models in future development programs.

The controls of the base engine and HPDI fuel system have now been fully integrated. Two ECMs operate the base engine and HPDI fuel system. Together with the new fuel pump, this now makes VIP control possible. VIP is a significant control lever for emissions. A portion of the later calibration work required mapping the optimal injection pressure over the engine's operating range.

After the new engine was commissioned and broken in, an AVL 8-mode test was run using the same settings as on the previous engine. The response of the new engine was very similar to that of the old engine, so all previous calibration work was directly transferable to this new engine.

Figure 49: New Engine Installed in Test Cell

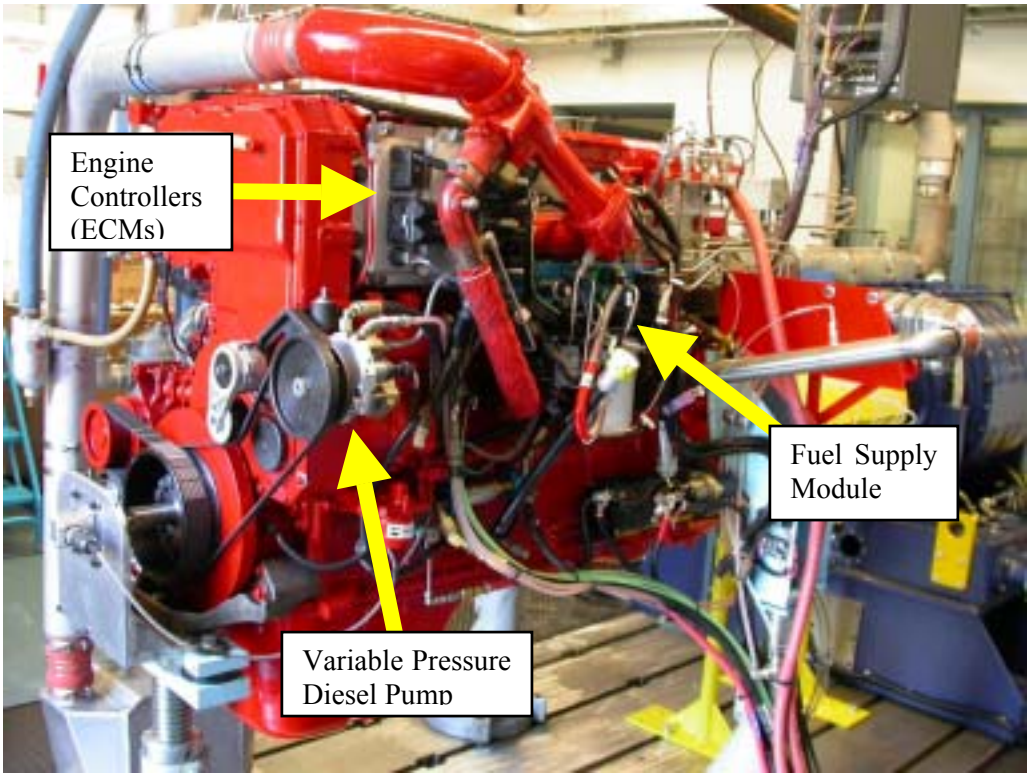

Figure 50: New Engine with Westport Production-Intent Fuel System and Controls

EGR Distribution and Measurement

The EGR rate, including the cylinder-to-cylinder variation, affects combustion and emissions. The engine head was instrumented to quantify the EGR distribution and its effects.

The engine controls use the overall EGR rate as an input, so this measurement must be accurate. The best bulk EGR sampling technique and location was to be found by EGR distribution measurements. Accurate EGR measurements were later used to calibrate the engine EGR sensor.

In the test cell, the EGR rate is calculated by measuring the CO_2 concentration in the charge flow and comparing it with that in the intake air and exhaust. The engine was instrumented for sampling CO_2 in the head and intake air horn. A top view schematic of the sample locations in the head and their relative position to the cylinder intake runners is shown in Figure 51.

The probe in position #1 was installed in the intake air horn (Figure 52) to measure the EGR fraction entering the intake manifold; this location was initially assumed to represent the average EGR rate. The probe has 12 evenly-spaced holes along the 0.25-in tube (three holes in three radial planes at four locations along the length of the tube).

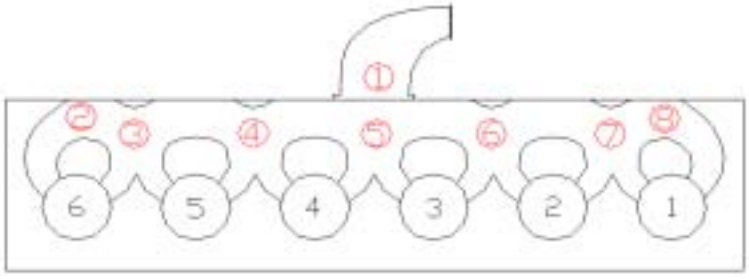

Figure 51: Top View Schematic of Head Showing Cylinders, Intake Runners, and EGR Sample Locations

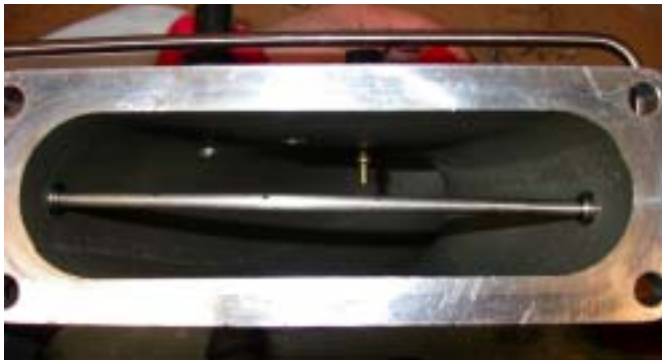

Figure 52: EGR Probe #1 in Intake Air Horn

Sampling locations 2-8 were as close as possible to the cylinder intake runners. Adjacent cylinders shared intake runners, so the probes did not necessarily indicate the EGR rate for particular cylinders. The measurements provided only a trend of the EGR distribution in the head.

Two sampling extraction methods were used. The first was a 0.25-in hole in the bottom of the intake manifold. The second was a “pepper pot” probe (Figure 53) sampling from the core of the charge. This probe consisted of a 0.25-in tube with 12 holes on three radial planes.

Figure 53: Typical “Pepper Pot” Sample Probe Installed in Cylinder Head

All sample lines were routed to a switching manifold (Figure 54) consisting of eight solenoid valves. This allowed sequential measurement from the individual locations or any combination of sample locations while the engine was operating. For labeling purposes, the sampling locations were labeled “probe 0” through “probe 8” where probes 1-8 represented each location in the head and intake air horn, and probe 0 was a descriptor for sampling a mixture from all locations at the same time.

Figure 54: EGR Sample Switching Manifold

After nearly 50 hours of operation, the probes were removed and testing continued with the flush-mount sampling. The carbon build-up on the probes over this time is shown in Figure 55, with cylinder 1 on the left through to cylinder 6 on the right. The relative blackening observed may indicate higher EGR rates to the middle cylinders.

Figure 55: EGR Sampling Probes after 50 Hours of Operation

To study the EGR distribution, the engine was run at various speeds and loads with the EGR flow held constant at each condition. Typically, the EGR valve was opened 70% or more. At each condition, a CO_2 measurement was taken at each sample location to determine the EGR fraction at that location. Over 450 tests were conducted so the data could be analyzed statistically.

A comparison of the average EGR fraction, over the range of speeds and loads, at each sample location is shown in Figure 56. The trends of the data are similar with and without the “pepper pot” probe. The tolerance bars represent +/- 1 standard deviation. Their wider ranges for the “probe” cases do not represent greater measurement error; they merely show that tests with the “pepper pot” probes were run over a wider range of EGR rates.

The difference between the EGR rate at each sample location and the average of the in-head locations is shown in Figure 57. Typically, the EGR fraction at probes 2 and 3 (near cylinders 6 and 5 respectively) was the lowest, whereas the EGR fraction at probes 7 and 8 (cylinders 2 and 1 respectively) was the highest.

These tests show less EGR near cylinders 5 and 6. To this point, the best sampling location and technique was probe location 5 (at the base of the intake manifold between cylinders 3 and 4) with a flush-mounted probe. All further testing used this method and sample location.

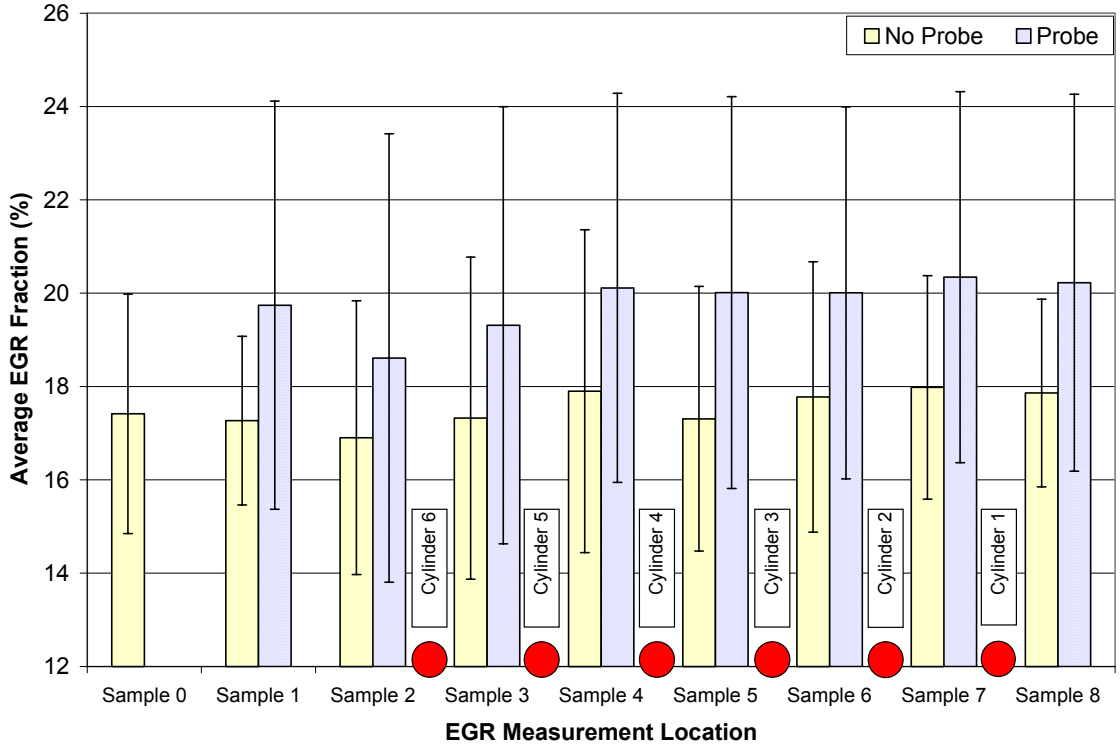

Figure 56: Average EGR Fraction at Each Sample Location over Various Speed-Load Conditions; Red Dots Show Cylinder Location Relative to Sample Location (466 Samples Total)

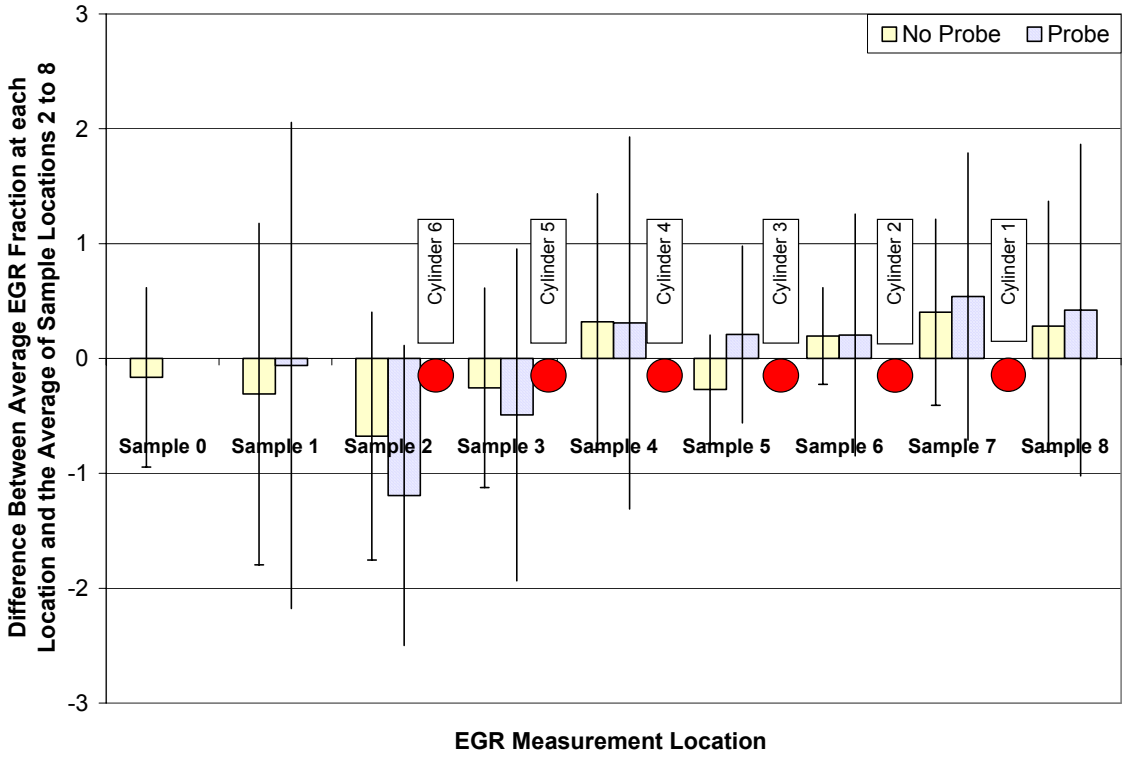

Figure 57: Difference Between EGR Fraction Determined from Sample Locations and Average of Sample Locations 2-8

Extra EGR Cooling

Earlier testing indicated that better EGR cooling would further reduce NO_x emissions by 10%-20% by allowing higher EGR rates (because cooler EGR occupies less volume) and by running with a lower inlet manifold temperature. A second EGR cooler was installed in series with the original (Figure 58 and Figure 59). This was only a demonstration and is not yet practical for vehicle installation.

The engine was again tested over the AVL 8-mode test. The extra EGR cooling reduced the cycle-weighted NO_x emissions by 10% but increased the CO and hydrocarbon emissions.

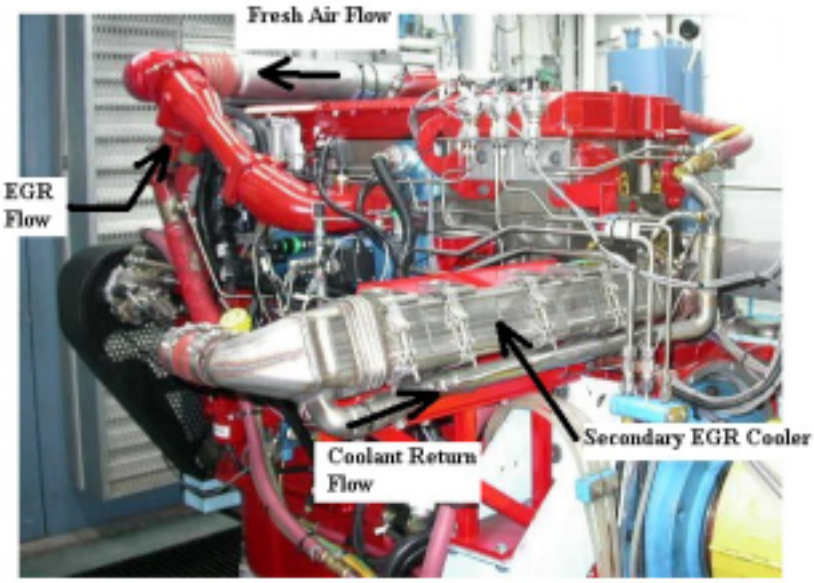

Figure 58: Second EGR Cooler Mounted in Series with Original Cooler

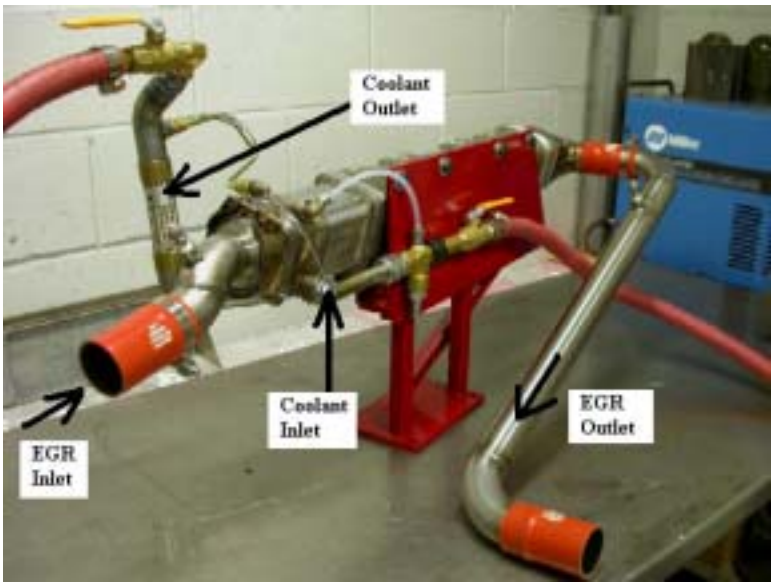

Figure 59: Second EGR Cooler

These initial tests were very promising. However, because test cell water was used in the extra cooler, the EGR was too cold, lower than the dew point at some modes, resulting in water condensation. Figure 60 shows the EGR temperature with and without the extra cooler. The coolant is typically just above 80°C, above the dew point at all modes.

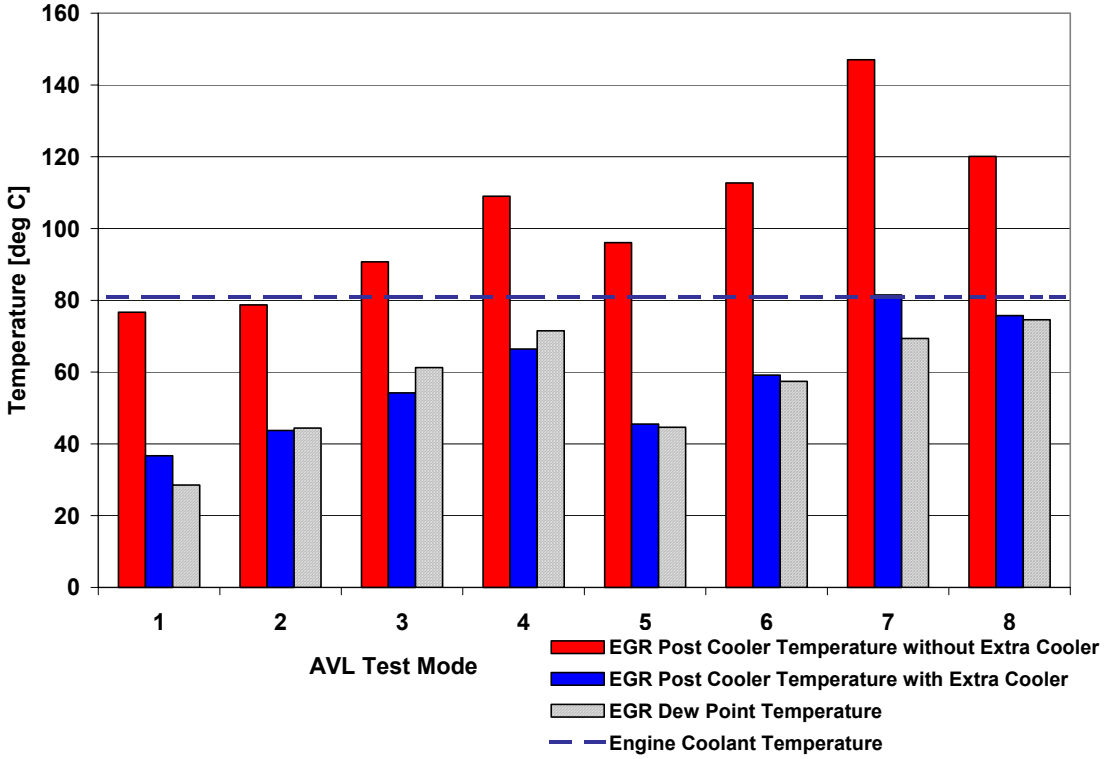

Figure 60: Cooled EGR Temperatures with and without the Extra EGR Cooler

To correct this, the cooling was altered so that the second cooler was cooled by engine coolant, in parallel with the primary cooler. Coolant for the secondary cooler was taken from the engine water pump and returned to the thermostat housing. This did not adversely affect the overall engine coolant system. This was the final configuration for the engine testing and calibration.

3.8 Optimization and Calibration Refinement

3.8.1 Objective

The objective was to optimize and calibrate the maps in the ECM to achieve the program goals of 0.5 g/bhp-hr NO_x, less than 0.1 g/bhp-hr PM, and greater than 40% peak thermal efficiency. This objective was to be achieved by means of steady-state and transient calibration.

3.8.2 Accomplishment Summary

All tests were conducted with the final engine hardware: the turbocharger with a smaller trim compressor, two EGR coolers, and an oxidation catalyst. The oxidation catalyst used earlier was re-installed because the exhaust backpressure affects engine operation.

More multi-parameter testing led to response surface models (RSMs) at each of 31 speed-load conditions. Engine settings selected from these models were validated by setting them manually in engine tests. Engine control maps were created with the results of these manual validation tests, and the same conditions were tested again with the engine running in an "automatic" mode. The engine was then tested over the ESC and AVL test modes with an oxidation catalyst.

The final steady-state engine calibration resulted in weighted NO_x emissions of 0.52 g/bhp-hr over the AVL 8-mode test and 0.36 g/bhp-hr over the ESC 13-mode test. The weighted PM over the ESC test was 0.04 g/bhp-hr, with a weighted thermal efficiency of 36.2% and a peak thermal efficiency of 39.5%. The weighted pilot fuel contribution to the overall weighted fuel consumption was 6% and 8.3% on the ESC and AVL test cycles, respectively

The engine, in its final hardware configuration, was shipped to the Cummins Engine Company, and the transient testing and calibration refinement were conducted there. Thirty-four FTP hot cycle tests were conducted with minor modifications of the engine calibration between tests.

3.8.3 Accomplishment Details

Steady-State Calibration: DoE Testing

Design of Experiments (DoE) is a technique for designing and analyzing experiments for maximum efficiency. Statistical analysis and regression are used to produce mathematical models of the responses (results of interest such as emissions and fuel consumption) in terms of the inputs (e.g., EGR rate, gas pressure, and SOI timing). After these models are created with a few well-chosen engine tests, the engine can be "virtually tested" on the computer by use of these models to find optimum settings and predict the response values.

To calibrate the engine, DoE testing was conducted at 31 points throughout the load-speed range of the engine, including the 13 ESC points and others (Figure 61).

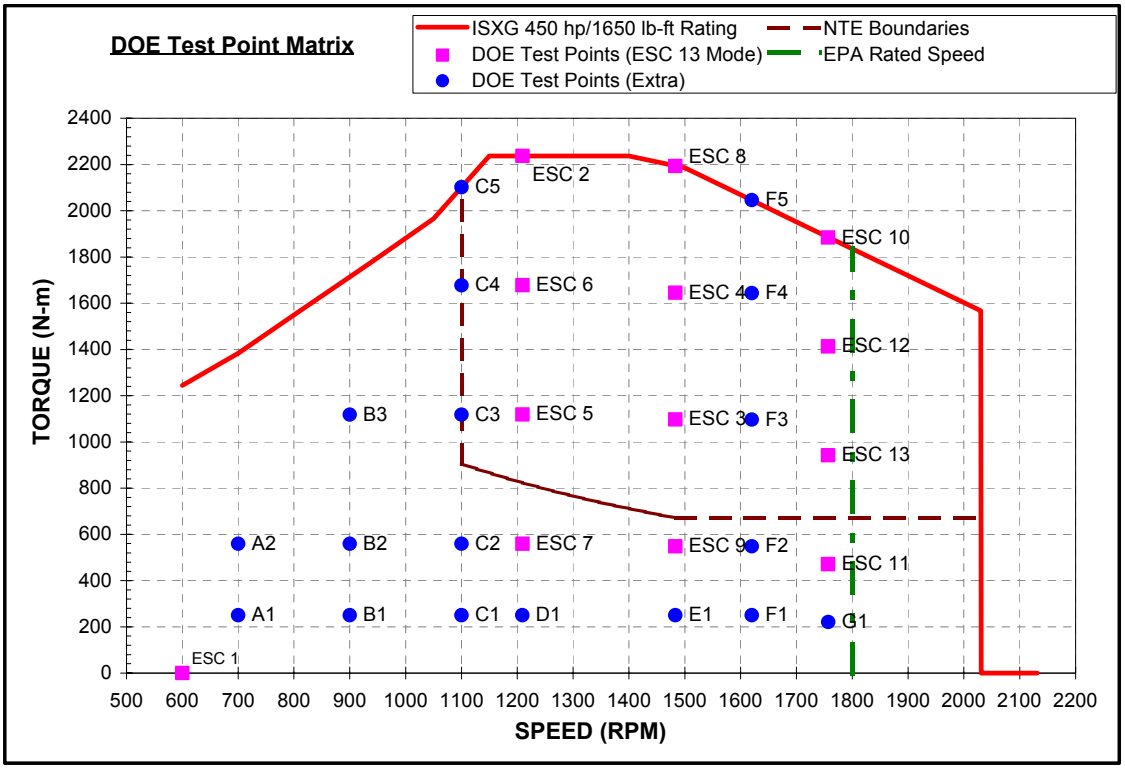

Figure 61: Calibration Test Points under the 450 hp/1,650 ft-lb Torque Curve

Earlier testing showed that the following are the main levers for control of emissions and fuel consumption:

- Gas start of injection (GSOI)
- Diesel fuel pressure
- EGR valve position
- VGT ring gap
- Pilot fueling quantity
- Pilot separation timing (before gas injection)

Earlier tests showed that it is unnecessary to vary all six levers at each point. Pilot separation and fueling were held at 800 µs and 10mg/stroke, respectively, because they have little effect on NO_x. The turbine ring gap remained closed at low load. The EGR valve was fully open at high speed/load points. Parameter ranges were chosen based on earlier results. A total of 677 tests were run: 15 modes with four parameters (27 points each) and 16 modes with three parameters (17 points each).

Steady-State Calibration: RSMs

Using DoE, test results were used to develop RSMs of emissions and fuel consumption at each test point. With RSMs, it was possible to develop trade-offs between different emission responses and fuel consumption, to aid later calibration optimization. The RSM analysis at each of the 31 test points was very similar, so only the analysis of a single test point (ESC mode 2, 1,209 rpm, 100% load) is presented here as a demonstration.

RSM Analysis Example: ESC Mode 2

Only three of the six control parameters were varied at ESC mode 2. Previous testing showed that the EGR valve should remain at 100% and that the pilot fueling and separation have little effect on emissions. Therefore, these parameters were held at 10 mg/stroke and at 800 µs, respectively. The variable factors and their ranges are shown in Table 6.

Table 6: ESC Mode 2—DoE Parameters and Ranges

Level	GSOI (°BTDC)	Turbine Ring Gap (mm)	Diesel Fuel Pressure (bar)
Max	8	8.5	260
Mid	6	7.5	240
Min	4	6.5	220

The RSMs were fitted to the test data. The models were used to find the minimum $BSNO_x$ at a given BSFC (Figure 62). Only one response can truly be minimized at a time. Consequently, the $BSCH_4$ and BSCO shown in Figure 62 are not minimized; they are merely the emissions resulting from this strategy of minimizing NO_x at a given BSFC.

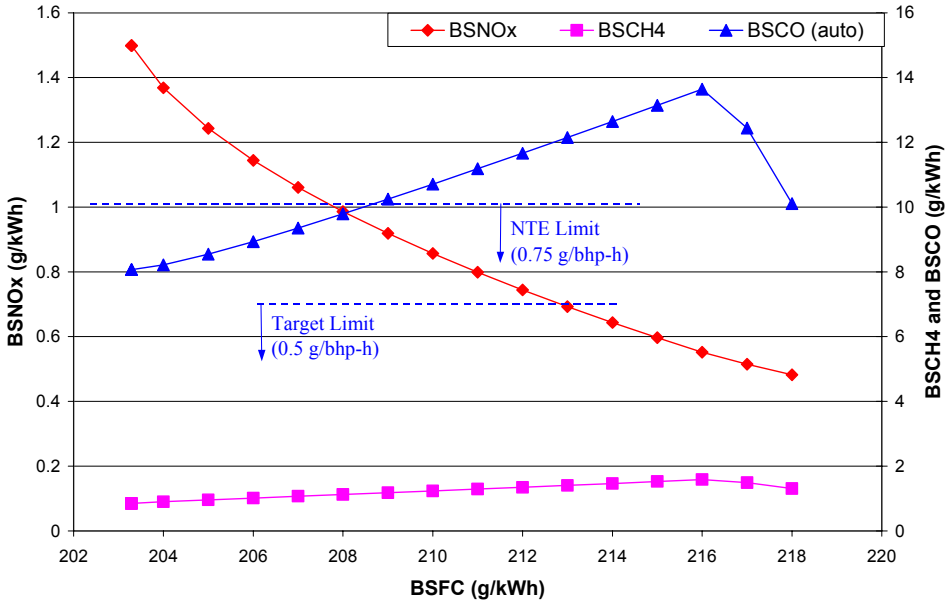

Figure 62: Minimized $BSNO_x$ vs. BSFC Tradeoff and Associated CH_4 and CO at ESC Mode 2

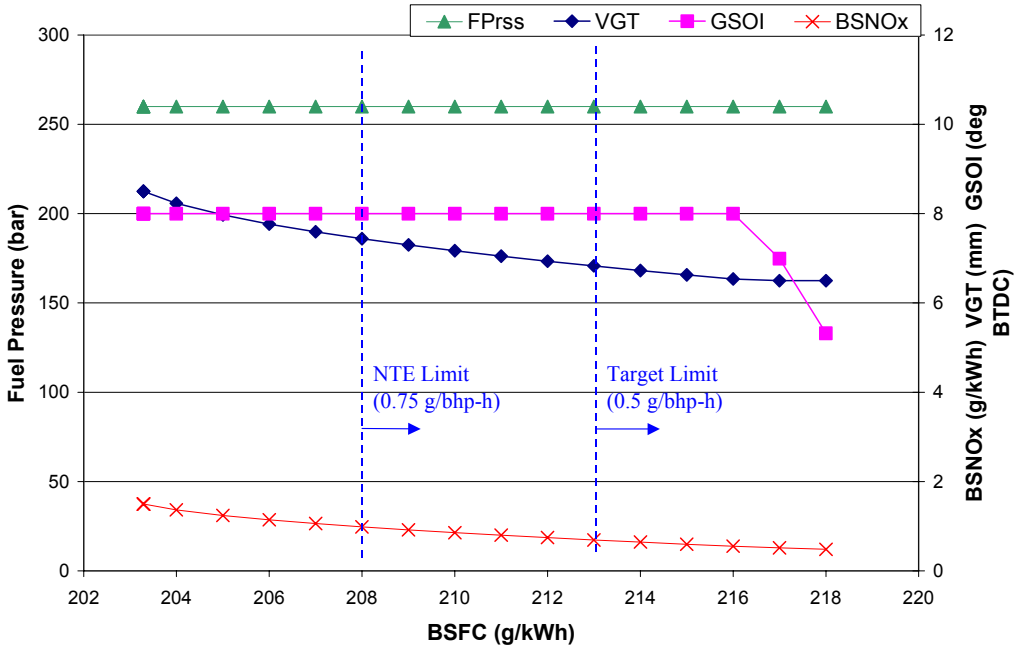

Figure 63: Engine Settings for Minimized $BSNO_x$-BSFC Tradeoff Curve at ESC Mode 2

The engine settings required to create this $BSNO_x$-BSFC tradeoff curve are shown in Figure 63. The fuel pressure should remain as high as possible and timing should remain advanced. As the VGT ring gap is reduced, which increases the exhaust backpressure and drives more EGR, the NO_x is reduced but with a BSFC penalty. When the VGT ring gap is as closed as possible (for the parameter ranges for this test), then NO_x may be reduced by retarding the timing.

Contour plots of the RSMs are shown in Figure 64 through Figure 67. Their shapes and slopes show how the responses are affected by the control parameters. For the parameter ranges of this test, CH_4 and CO are insensitive to fuel pressure. NO_x is strongly affected by VGT ring gap because as the ring gap is decreased the exhaust pressure increases, driving more EGR.

Although the optimized settings shown in Figure 63 suggest operating at advanced timings and a closed VGT ring gap, the CO is very high at these conditions. Figure 68 shows that retarding the timing would reduce the CO greatly with a small BSFC penalty at a constant NO_x emission. For example, at 0.5 g/bhp-h NO_x, retarding the timing from 8 to 4 degrees reduces CO by 50% while only increasing BSFC by 0.5%. Figure 67 also indicates that CO can be reduced by opening the VGT slightly, which would also reduce the possibility of turbo surge.

Therefore, the following are the probable operating conditions suggested by the RSM for ESC mode 2:

- High fuel pressure (260 bar) to reduce BSFC
- Turbine ring gap as closed as possible without increasing CO excessively or approaching surge region of compressor (~7 mm)

- Retarded GSOI (4 to 6 degrees BTDC) to reduce CO and smoke while avoiding combustion instability and excessive exhaust temperatures

Similar conclusions and graphs were made for each DoE test point. In general, at low speed and load points, fuel pressure is low, EGR valve position is around 30% open, and GSOI is retarded. As speed and load increase, fuel pressure increases, the EGR valve opens, and GSOI advances to accommodate the longer burn caused by the increased EGR. The turbine ring gap is fully closed for low load conditions and opens as load increases to prevent combustion instability and surge while still maintaining enough exhaust backpressure to drive sufficient EGR.

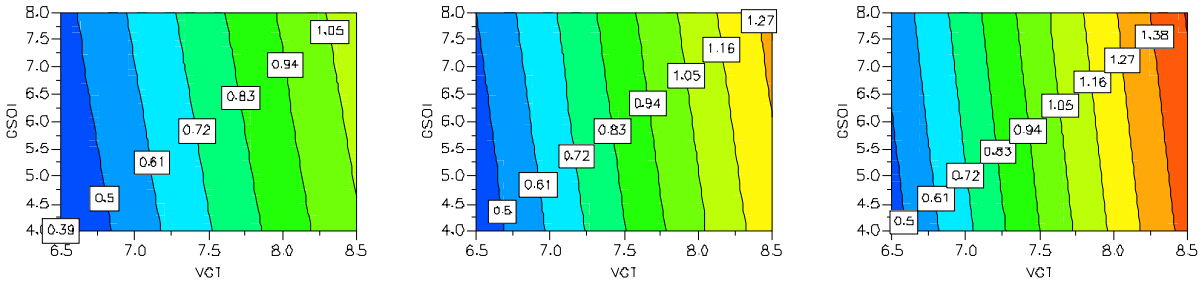

Fuel Pressure = 220 Fuel Pressure = 240 Fuel Pressure = 260

Figure 64: Contour Plots of $BSNO_x$ RSM at ESC Mode 2 (Units: $BSNO_x$ = g/bhp-hr, Fuel Pressure = bar, GSOI = degrees BTDC, VGT = mm)

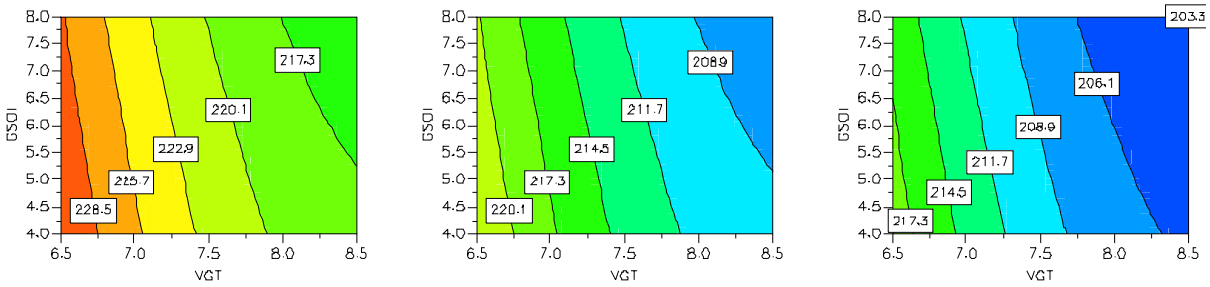

Fuel Pressure = 220 Fuel Pressure = 240 Fuel Pressure = 260

Figure 65: Contour Plots of BSFC RSM at ESC Mode 2 (Units: BSFC = g/bhp-hr, Fuel Pressure = bar, GSOI = degrees BTDC, VGT = mm)

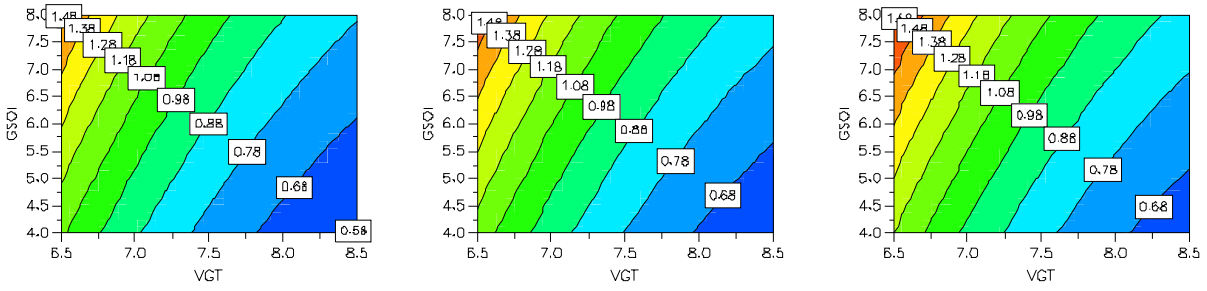

Fuel Pressure = 220 Fuel Pressure = 240 Fuel Pressure = 260

Figure 66: Contour Plots of $BSCH_4$ RSM at ESC Mode 2 (Units: $BSCH_4$ = g/bhp-hr, Fuel Pressure = bar, GSOI = degrees BTDC, VGT = mm)

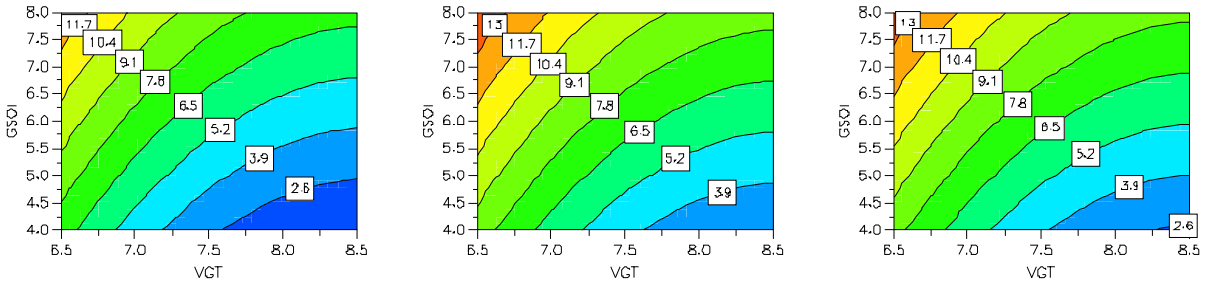

Fuel Pressure = 220 Fuel Pressure = 240 Fuel Pressure = 260

Figure 67: Contour Plots of BSCO RSM at ESC Mode 2 (Units: BSCO = g/bhp-hr, Fuel Pressure = bar, GSOI = degrees BTDC, VGT = mm)

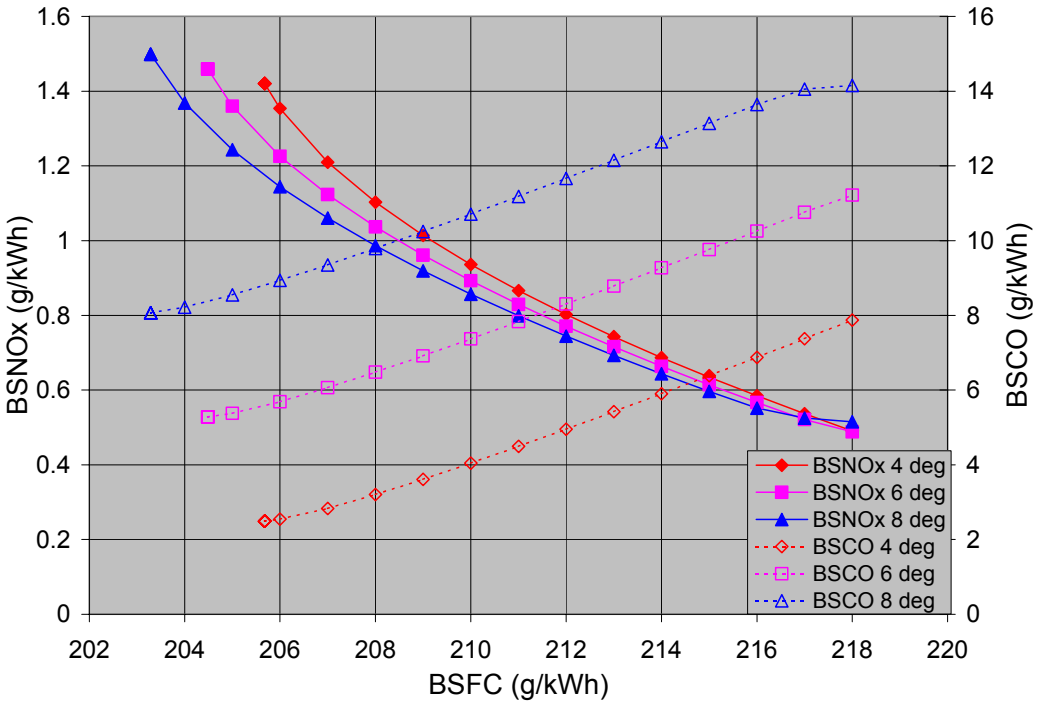

Figure 68: Minimized $BSNO_x$ and BSCO vs. BSFC at Various GSOI Settings at ESC Mode 2

Steady-State Calibration Development

The optimal parameter settings at different engine operating conditions were selected using the results of the RSMs. Settings were selected based on the following criteria:

- Minimize $BSNO_x$ (especially in NTE region of engine map)
- Maximize efficiency
- Maintain exhaust opacity levels well below visible limit
- Do not exceed engine hardware limits (exhaust temperature, turbo speed, compressor outlet temperature, coolant temperature, etc.)
- Minimize CO and CH_4 emissions

The engine was run at the DoE test points with the engine parameters set manually at the optimal settings. Data from these tests were used to create maps for the engine controller.

The resulting calibration allowed the engine to run automatically. The engine was run over the ESC 13-mode points, and the resulting automatic parameter settings were compared with the manual settings. If the automatic settings were not achieving their targeted settings, the engine calibration was modified and then tested again. Some of the targeted settings were modified slightly from the original manual settings. The steady-state calibration was considered complete when it met the desired parameter settings repeatedly during automatic operation.

The ESC 13-mode test was run twice with the final steady-state calibration to measure pre- and post-catalyst emissions (results presented below). The engine settings and operating conditions in the manual and automatic tests are compared in Figure 69 through Figure 74.

The automatic gas SOI and fuel pressure (Figure 69 and Figure 70) generally match the manually set conditions. The EGR fraction (Figure 74) is generally higher than the manually set conditions at all test modes, the result of changes to the calibration. This increase in the EGR fraction is reflected in the VGT ring gap setting (Figure 71), which is consistently smaller than the manually set conditions.

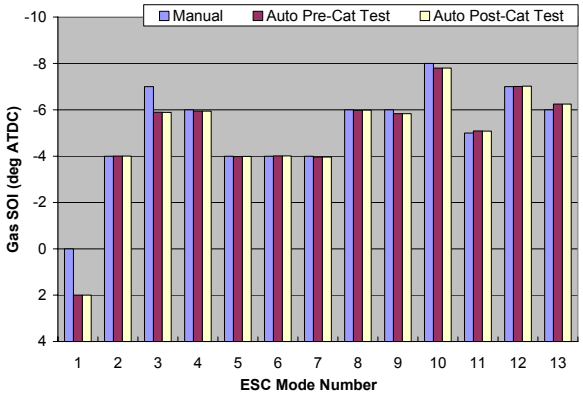

Figure 69: Gas SOI Comparison—Manual vs. Automatic

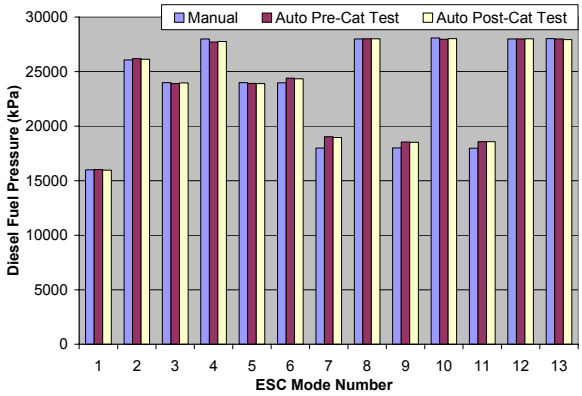

Figure 70: Fuel Pressure Comparison—Manual vs. Automatic

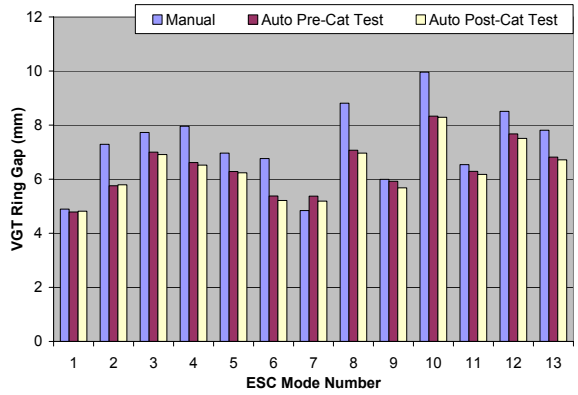

Figure 71: VGT Ring Gap Comparison—Manual vs. Automatic

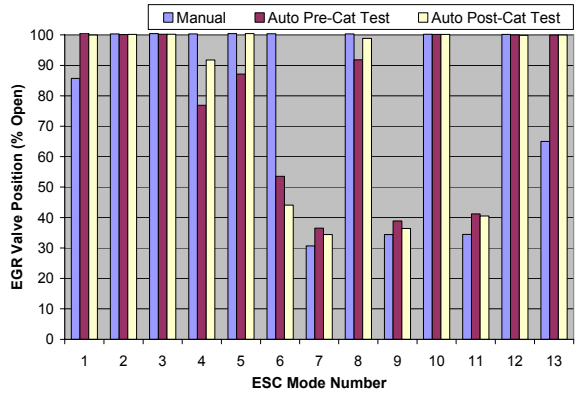

Figure 72: EGR Valve Position Comparison—Manual vs. Automatic

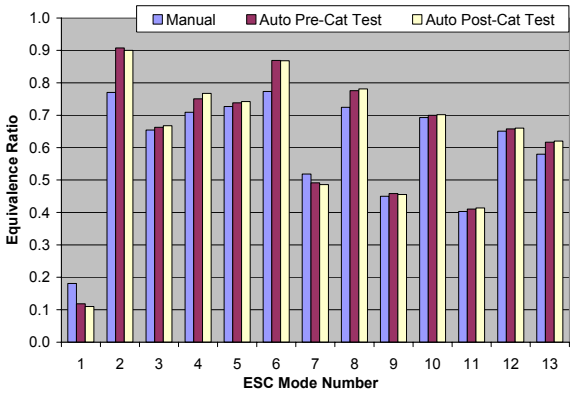

Figure 73: Equivalence Ratio Comparison—Manual vs. Automatic

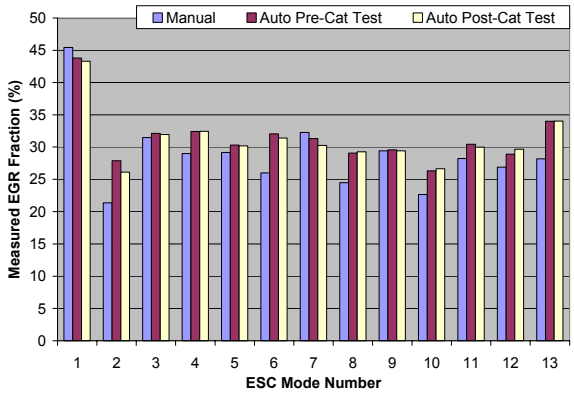

Figure 74: Measured EGR Fraction Comparison—Manual vs. Automatic

Final Steady-State Test Results: ESC 13 Mode

The ESC 13-mode test was run automatically with the final steady-state calibration for pre- and post-catalyst emissions; results are shown in Table 7. The weighted NO_x was 0.36 g/bhp-hr, much lower than the target of 0.5 g/bhp-hr, and the weighted PM was 0.04 g/bhp-hr. The weighted brake specific NMHC (BSNMHC) was 0.2 g/bhp-hr, about 9% of the total hydrocarbons (HC) emissions. The catalyst had the greatest effect on CO and NMHC. It should have little effect on NO_x, so any variation is likely due to measurement error. The pre- and post-tests were run on different days.

On an energy basis, the ESC-weighted diesel pilot was 6% of total fuel consumption. At high load, it accounts for less than 5%.

Table 7: Final ESC 13-Mode Emissions Results

ESC Mode	Speed (rpm)	Load (%)	Test	BSNOx (g/bhp-h)	BSnmHC (g/bhp-h)	BSCO (g/bhp-h)	BSCH4 (g/bhp-h)	BSFC (g/bhp-h)	BTE (%)	PM (g/bhp-h)
2	1209	100	Pre	0.17	0.30	10.19	1.24	169.1	37.1	-
			Post	0.21	0.09	0.00	1.01	168.6	37.2	0.077
3	1483	50	Pre	0.36	0.42	3.58	2.68	166.1	37.7	-
			Post	0.36	0.26	0.01	2.88	167.6	37.4	0.069
4	1483	75	Pre	0.26	0.32	6.13	1.97	166.4	37.7	-
			Post	0.25	0.19	0.01	2.10	168.2	37.2	0.052
5	1209	50	Pre	0.35	0.29	2.58	1.64	158.8	39.5	-
			Post	0.33	0.17	0.01	1.83	160.0	39.2	0.034
6	1209	75	Pre	0.15	0.59	9.32	3.12	173.2	36.2	-
			Post	0.17	0.18	0.01	2.19	172.6	36.3	0.024
7	1209	25	Pre	0.79	0.50	2.44	2.97	169.0	37.1	-
			Post	0.76	0.29	0.01	3.08	166.1	37.7	0.012
8	1483	100	Pre	0.28	0.25	5.86	1.23	170.4	36.8	-
			Post	0.29	0.11	0.01	1.16	170.2	36.8	0.024
9	1483	25	Pre	0.84	0.52	2.36	3.11	182.8	34.3	-
			Post	0.79	0.32	0.01	3.38	182.6	34.3	0.008
10	1757	100	Pre	0.36	0.25	4.59	1.10	176.1	35.6	-
			Post	0.37	0.13	0.01	1.29	176.7	35.5	0.006
11	1757	25	Pre	0.80	0.81	3.80	5.43	213.0	29.4	-
			Post	0.78	0.55	0.01	5.91	215.7	29.1	0.006
12	1757	75	Pre	0.37	0.30	3.48	1.80	173.1	36.2	-
			Post	0.36	0.20	0.01	2.02	173.9	36.0	0.012
13	1757	50	Pre	0.35	0.62	4.12	4.36	181.0	34.6	-
			Post	0.34	0.45	0.01	4.78	182.3	34.4	0.007
Composite Results			Pre	0.352	0.366	5.581	2.032	172.9	36.2	-
			Post	0.357	0.198	0.010	2.075	173.4	36.1	0.040

Final Steady-State Test Results: AVL 8 Mode

The AVL 8-mode test was run automatically with the final steady-state calibration for pre- and post-catalyst emissions; results are shown in Table 8. PM emissions were not recorded because they were measured during the subsequent transient testing.

The weighted $BSNO_x$ was 0.52 g/bhp-hr, near the target of 0.5 g/bhp-hr. The weighted BSNMHC was 0.22 g/bhp-hr, which accounted for about 8% of the total HC emissions. On an energy basis, the weighted diesel (pilot) use was 8% of total fuel consumption.

Table 8: Final AVL 8-Mode Emissions Results

AVL Mode	Speed (rpm)	Load (%)	Test	BSNOx (g/bhp-h)	BSnmHC (g/bhp-h)	BSCO (g/bhp-h)	BSCH4 (g/bhp-h)	BSFC (g/bhp-h)	BTE (%)
2	732	25	Pre	1.17	0.55	3.22	3.37	182.3	34.4
			Post	0.82	0.31	0.01	4.05	171.7	36.5
3	854	63	Pre	0.49	0.24	5.79	0.83	160.3	39.1
			Post	0.41	0.07	0.00	0.92	166.2	37.7
4	984	84	Pre	0.29	0.21	9.72	0.68	165.2	37.9
			Post	0.26	0.05	0.00	0.61	164.6	38.1
5	1800	18	Pre	1.32	0.81	4.15	5.45	263.7	23.8
			Post	1.16	0.49	0.02	6.41	254.1	24.7
6	1740	40	Pre	0.58	0.41	2.88	3.22	182.8	34.3
			Post	0.56	0.28	0.01	3.74	181.4	34.5
7	1740	69	Pre	0.35	0.30	4.11	2.09	174.1	36.0
			Post	0.36	0.18	0.01	2.30	172.2	36.4
8	1668	95	Pre	0.31	0.26	6.18	1.11	176.8	35.4
			Post	0.31	0.11	0.01	1.35	175.7	35.7
Composite Results			Pre	0.554	0.372	5.067	2.227	186.2	33.7
			Post	0.523	0.219	0.017	2.568	184.8	33.9

Steady-State Test Results: Heat Release Analysis

At the AVL and ESC test points, the peak cylinder pressures are well below the rated maximum cylinder pressure. The start of gas combustion is typically a few degrees past the angle of maximum cylinder pressure, whereas the 50% burn angle for most points is about 15-20 degrees ATDC. This is typical of low-NO_x engines. However, if the 50% burn angle were more advanced the efficiency could be improved. Examples of the cylinder pressure and heat release are shown in Figure 75 and Figure 76.

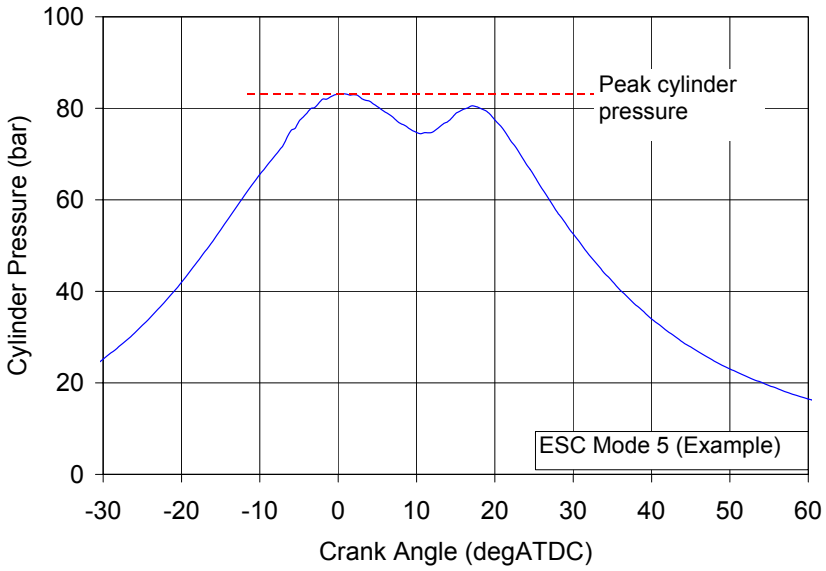

Figure 75: Example of In-Cylinder Pressure Measurement

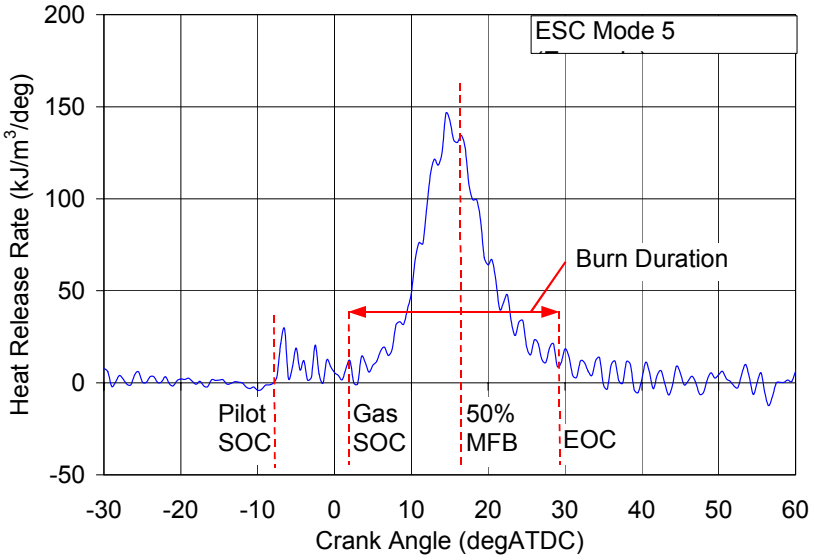

Figure 76: Example of Heat Release Rate from In-Cylinder Pressure Measurement

Transient Calibration Development

The engine in its final configuration was installed in a transient test cell at Cummins' facilities in Columbus, Indiana. Transient calibration and testing were conducted concurrently. All transient testing and calibration only involved running complete hot-cycle FTP tests. Snap tests for acceleration or simulated gear changes were not conducted because these are included in the FTP test. The FTP is a 20-min test with sections that simulate typical light urban traffic with stops and starts, crowded urban traffic with few stops, and crowded expressway traffic (Figure 77).

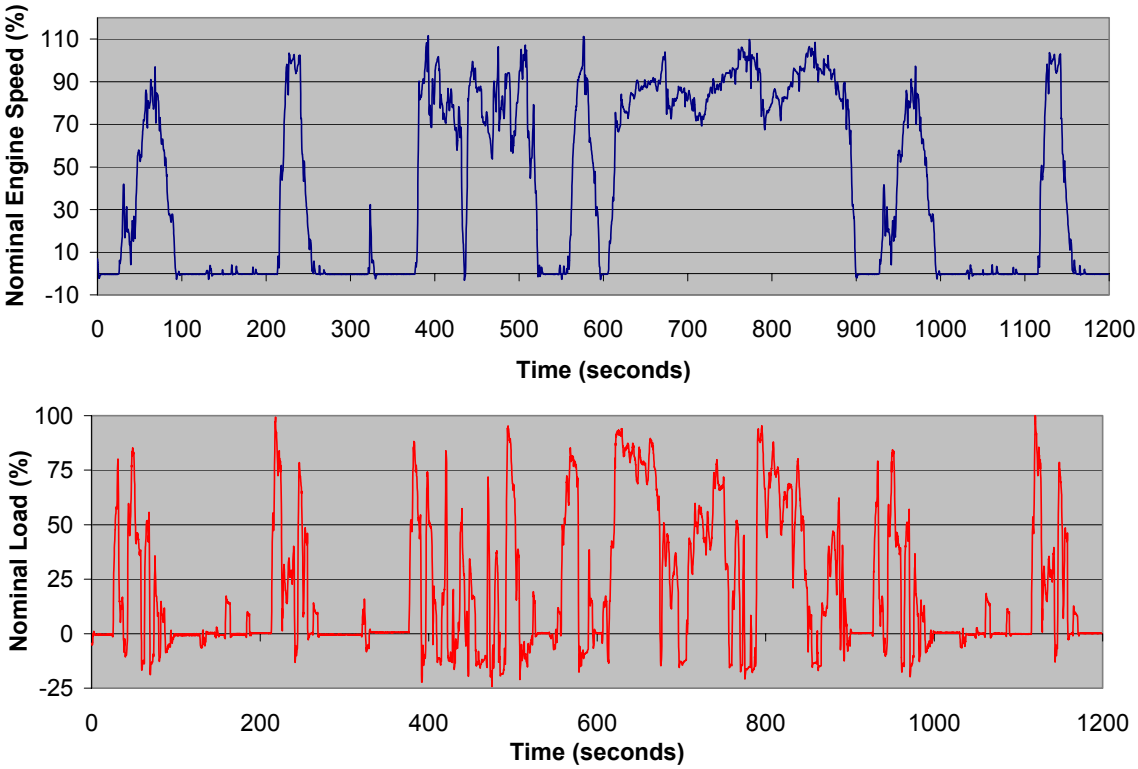

Figure 77: FTP Transient Speed and Load Profile

The FTP test points are calculated from the engine's torque curve, which must be measured first. During this torque curve test, the engine is loaded to 100%, and the speed is increased from idle to the governed speed at 8 rpm/s. The resulting measured torque is the basis for determining the subsequent FTP test points. The measured torque curve and the advertised 450 hp/1,650 ft-lb torque curve are compared in Figure 78. The two torque curves match very well.

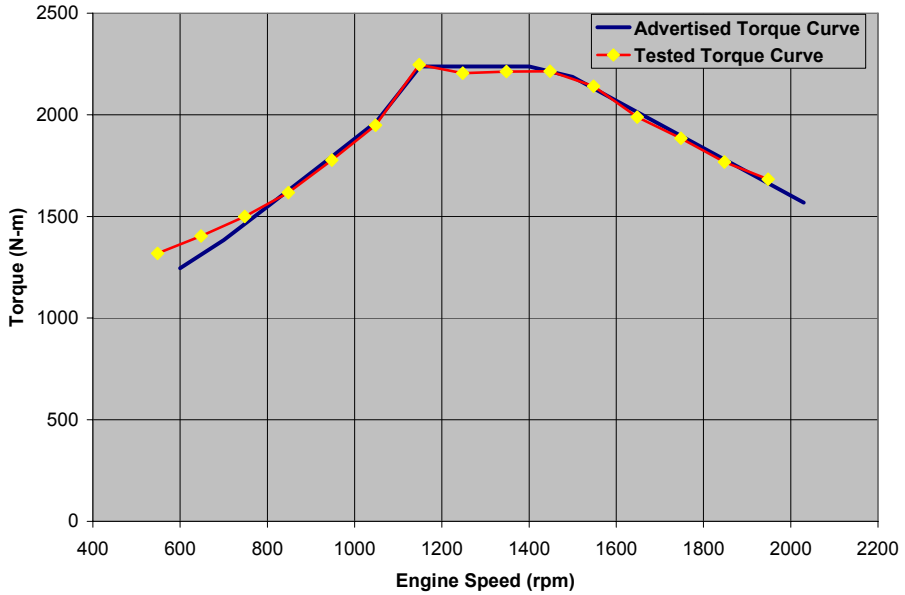

Figure 78: Target 450 hp (1,650 ft-lb/2,237 N-m) Torque Curve and Tested Torque Curve

During the FTP, the engine must follow the demanded speed and torque closely. To confirm this, every second the actual speed, torque, and power are recorded, along with the corresponding target values. After the test, the target and actual values are compared in a linear regression. All results presented here have passed the statistical requirements.

The first series of FTP tests resulted in $BSNO_x$ emissions of 0.7-0.8 g/bhp-hr with BSHC emissions of 2.4-2.8 g/bhp-hr. These tests were run with the calibration used in the earlier ESC and AVL steady-state tests. This was the starting point for developing the transient calibration.

Analysis of the transient data suggested the main techniques for reducing the transient emissions:

- Increase the demanded EGR fraction
- Increase the EGR fraction during acceleration because the EGR valve shuts to help increase the fresh air content during rapid rises in fueling rate
- Reduce the fuel pressure because the dynamic response of the fuel system is slow and high fuel pressures cannot be reduced quickly during decelerations
- Retard the fuel injection timing

Figure 79 shows the effect of these changes to the base calibration. Increasing the EGR fraction reduces the NO_x but with a penalty in HC. Retarding the timing globally does not reduce the NO_x appreciably but HC increases greatly, so this strategy was not used. Reducing the fuel pressure had a slight positive effect in reducing the NO_x. There was only a slight compounding effect when these strategies were combined. Although there was no speciation of the HC emissions, much of this is assumed to be CH_4 as was observed during the steady-state testing.

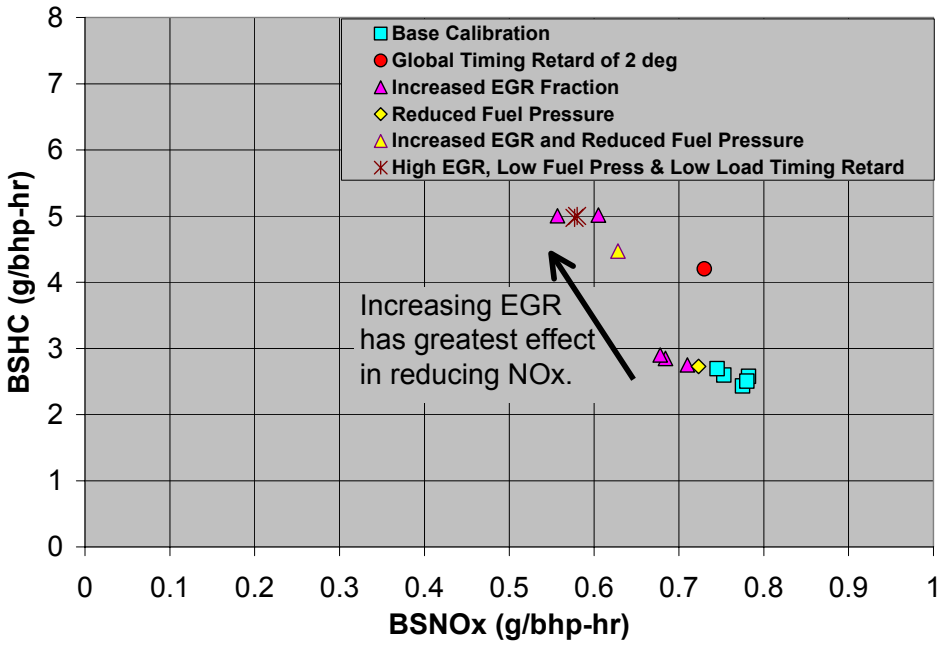

Figure 79: Transient Calibration Development

One contributor to the NO_x that could not be controlled effectively was the transient response of the EGR valve during rapid accelerations (Figure 80). During acceleration, the EGR valve closes rapidly and the NO_x emissions rise rapidly. As the control system responds, the EGR valve opens, the EGR fraction increases, and the NO_x decreases. This suggests that NO_x may be reduced further if the EGR fraction could be maintained or partially maintained during acceleration. Changes to the air handling system would be required to make this possible.

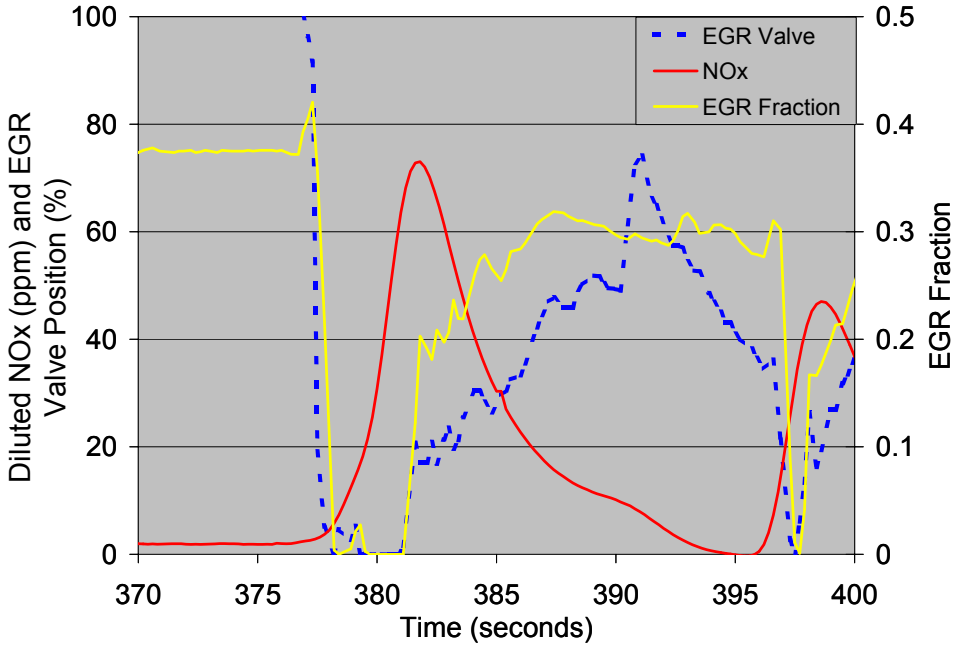

Figure 80: Transient NO_x, EGR Valve, and EGR Fraction Response during Rapid Acceleration

3.9 Transient Testing

3.9.1 Objective

The objective was to conduct transient engine tests according to FTP requirements and demonstrate emissions levels of the engine operating under automatic controls.

3.9.2 Accomplishment Summary

Thirty-four FTP hot-cycle tests were run with minor modifications to the calibration between tests. Average NO_x emissions of 0.6 g/bhp-hr were repeatedly demonstrated with a best result of 0.56 g/bhp-hr. The average PM emissions remained relatively constant at about 0.03 g/bhp-hr. The average BTE was 34.1%

3.9.3 Accomplishment Details

Transient FTP Results

The final calibrations resulted in average FTP NO_x emissions of 0.6 g/bhp-hr with a best result of 0.56 g/bhp-hr, while the BSHC emissions remained around 5 g/bhp-hr. The

NMHC portion of the HC emissions was not measured, but the steady-state test results suggest that NMHC is around 8%-9% of the total HC emissions. The average PM emissions remained relatively constant at around 0.03 g/bhp-hr. These final transient results are shown in Figure 81 and Figure 82. For the results shown in Figure 81, the standard deviation in the recorded NO_x measurement is about 0.03 g/bhp-hr.

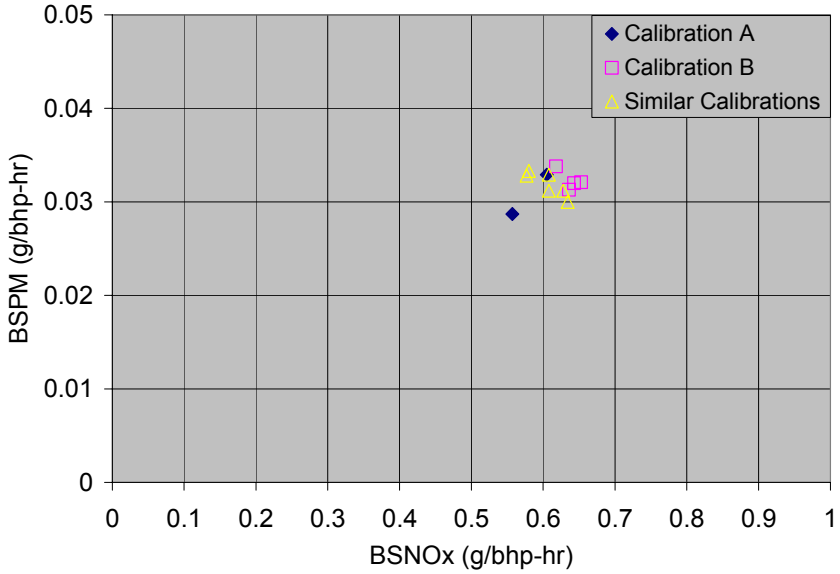

Figure 81: Final Transient FTP Tests—BSNO$_x$ vs. BSPM

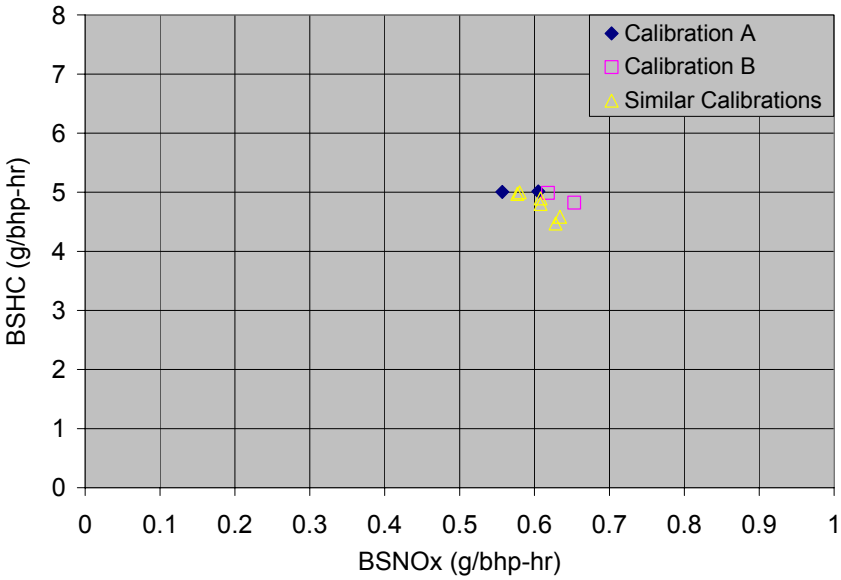

Figure 82: Final Transient FTP Tests—BSNO$_x$ vs. BSHC

Fuel consumption was not directly measured during the transient testing, but it was calculated from the emissions measurements. The average BTE for the final FTP tests was 34.1%. This value is comparable to state-of-the-art diesel engines, which typically report thermal efficiencies of 32%-35%. A plot of the BTE results is shown in Figure 83.

Because the fuel consumption was not measured, the pilot energy fraction of the total fuel consumption cannot be reported. However, because it was 6% on the ESC test cycle and 8% on the AVL test cycle, the pilot fuel contribution on the FTP is expected to be small.

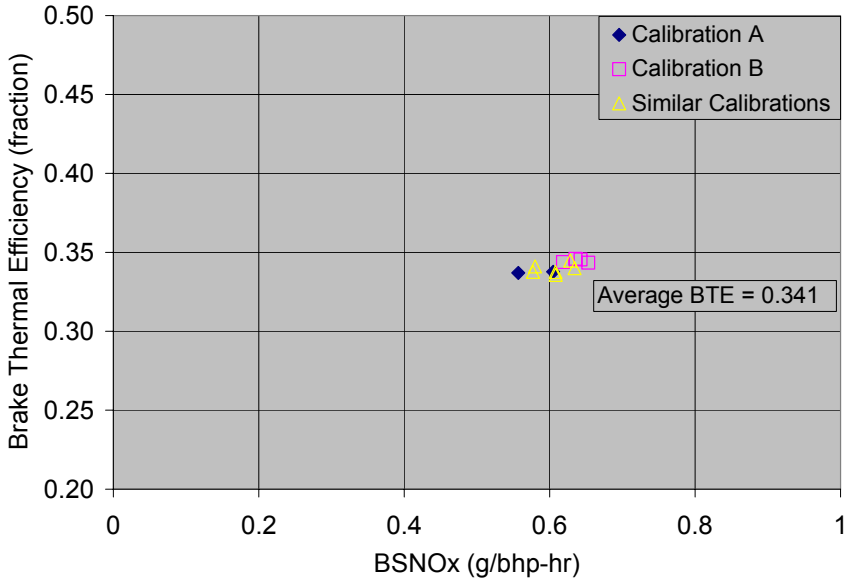

Figure 83: Final FTP Tests—BSNO$_x$ vs. BTE

4.0 Conclusions and Recommendations

The Westport HPDI natural gas fueling system, a second EGR cooler, a smaller trim turbocharger compressor, and an oxidation catalyst enable very significant emissions reduction to be achieved on the ISX platform. Diesel engine and emissions performance can be retained while reducing NO_x emissions to 0.6 g/bhp-hr and PM to 0.03 g/bhp-hr.

The testing and modeling results indicated that there are untried hardware changes that could improve performance and emissions:

- Install a smaller turbine (either VGT or wastegated) to increase EGR rates during transient conditions.
- Install the two EGR coolers in parallel so each receives half the mass flow. The current EGR flow rate exceeds the design capacity of the coolers. Alternately, a new single EGR cooler with a higher flow capacity could be used.
- Investigate control strategies that could assist NO_x control during transients.
- Improve the EGR mixing with the fresh air flow.
- Change the piston bowl geometry to better match the HPDI fuel injection process. This may improve HC, CO, and PM emissions.
- Refine the oxidation catalyst system to improve the cost/performance tradeoff, particularly for CH_4, ethane, and propane emissions.

5.0 References

1. Ouellette P., Douville B., Hill P.G., and Ursu B., "NO_x reduction in a directly injected natural gas engine," Proceedings of the 1998 Fall Technical Conference of the ASME, IC Engines Division, ICE Vol. 31-3, September 1998.
2. Harrington J., Munshi S., Nedelcu C., Ouellette P., Thompson J., Whitfield S., "Direct Injection of Natural Gas in a Heavy-Duty Diesel Engine," SAE Technical Paper 2002-01-1630, 2002.

REPORT DOCUMENTATION PAGE

Form Approved
OMB No. 0704-0188

PLEASE DO NOT RETURN YOUR FORM TO THE ABOVE ORGANIZATION.

1. REPORT DATE *(DD-MM-YYYY)*	2. REPORT TYPE	3. DATES COVERED *(From - To)*
May 2004	Subcontract Report	2003-2004

4. TITLE AND SUBTITLE
Development of the High-Pressure Direct-Injected, Ultra Low-NOx Natural Gas Engine: Final Report

5a. CONTRACT NUMBER
DE-AC36-99-GO10337

5b. GRANT NUMBER

5c. PROGRAM ELEMENT NUMBER

6. AUTHOR(S)
V.K. Duggal, E.J. Lyford-Pike, J.F. Wright, M. Dunn, D. Goudie, and S. Munshi

5d. PROJECT NUMBER
NREL/SR-540-35911

5e. TASK NUMBER

5f. WORK UNIT NUMBER

7. PERFORMING ORGANIZATION NAME(S) AND ADDRESS(ES)
Cummins, Inc.
Columbus, Indiana, USA
Westport Innovations, Inc.
Vancouver, British Columbia, Canada

8. PERFORMING ORGANIZATION REPORT NUMBER
NCI-1-31036-01

9. SPONSORING/MONITORING AGENCY NAME(S) AND ADDRESS(ES)
National Renewable Energy Laboratory
1617 Cole Blvd.
Golden, CO 80401-3393

10. SPONSOR/MONITOR'S ACRONYM(S)
NREL

11. SPONSORING/MONITORING AGENCY REPORT NUMBER
NREL/SR-540-35911

12. DISTRIBUTION AVAILABILITY STATEMENT
National Technical Information Service
U.S. Department of Commerce
5285 Port Royal Road
Springfield, VA 22161

13. SUPPLEMENTARY NOTES
NREL Technical Monitor: M. Frailey

14. ABSTRACT *(Maximum 200 Words)*
Subcontractor report details work done by Cummins and Westport Innovations to develop a heavy-duty, low-NOx, high-pressure direct-injection natural gas engine for the Next Generation Natural Gas Vehicle activity.

15. SUBJECT TERMS
cummins; westport; natural gas vehicle; hpdi; exhaust gas recirculation; egr; nox; ngngv; natural gas; lng; cng; high-pressure direct-injection; next generation natural gas vehicle; ngv; oxidation catalyst; heavy-duty; engine

16. SECURITY CLASSIFICATION OF:			17. LIMITATION OF ABSTRACT	18. NUMBER OF PAGES	19a. NAME OF RESPONSIBLE PERSON
a. REPORT	b. ABSTRACT	c. THIS PAGE			19b. TELEPONE NUMBER (*Include area code)*
Unclassified	Unclassified	Unclassified	UL		

Standard Form 298 (Rev. 8/98)
Prescribed by ANSI Std. Z39.18